The Appendix Orchestrates T-Cell Mediated Immunosurveillance in Colitis-Associated Cancer

Maxime Collard, Julien Tourneur-Marsille, Mathieu Uzzan, Miguel Albuquerque, Maryline Roy, Anne Dumay, Jean-Noël Freund, Jean-Pierre Hugot, Nathalie Guedj, Xavier Treton, et al.

The appendix orchestrates T-cell mediated immunosurveillance in colitis-associated cancer

Maxime K. Collard[1,2], Julien Tourneur-Marsille[2], Mathieu Uzzan[2,3], Miguel Albuquerque[4], Maryline Roy[2], Anne Dumay[2], Jean-Noël Freund[5], Jean-Pierre Hugot[2], Nathalie Guedj[2,4], Xavier Treton[2,3], Yves Panis[1,2], Eric Ogier-Denis[2,6]

[1] Assistance Publique Hôpitaux de Paris, Service de Chirurgie Colorectale, Hôpital Beaujon, Clichy, France.
[2] Université de Paris, Centre de Recherche sur l'Inflammation, INSERM, U1149, CNRS, ERL8252, "Gut Inflammation", Paris, France.
[3] Assistance Publique Hôpitaux de Paris, Service de Gastroentérologie, Hôpital Beaujon, Clichy, France.
[4] Assistance Publique Hôpitaux de Paris, Service d'Anatomopathologie, Hôpital Beaujon, Clichy, France.
[5] Université de Strasbourg, Inserm, IRFAC / UMR-S1113, FHU ARRIMAGE, ITI InnoVec, FMTS, 67200 Strasbourg, France
[6] INSERM, Université Rennes, CLCC Eugène Marquis, « Chemistry, Oncogenesis, Stress Signaling » UMR_S 1242, F-35000 Rennes, France

Corresponding author: Dr. Eric Ogier-Denis, INSERM 1149/1242, rue de la Bataille Flandres Dunkerque Bâtiment D 1er étage 3 RENNES, France, **Email**: eric.ogier-denis@inserm.fr

Short title: Appendectomy and colorectal cancer in UC

Word count : 3,825

Grant support: This work was supported by the recurrent operating grant of the French Institute of Health (INSERM), Université de Paris, Centre de Lutte contre le Cancer Eugène Marquis de Rennes, Région Bretagne et Rennes Métropole, Investissements d'Avenir programme (ANR-11-IDEX-0005-02), Sorbonne Paris Cité, Laboratoire d'Excellence Labex Inflamex, Fondation

de l'Avenir (AP-RM-17-008), la Ligue contre le Cancer (LCC) and Association François Aupetit (AFA).

Publication history: This manuscript was previously published in medRxiv, doi:10.1101/2021.05.25.21257681 under the title: "The appendix orchestrates T-cell mediated immunosurveillance in colitis-associated cancer".

Conflict of interest: The authors declare that there is no conflict of interest.

Abbreviations: AOM: azoxymethane; CAC: colitis-associated cancer; CRC: colorectal cancer; DSS: dextran sodium sulfate; IBD: inflammatory bowel disease; UC: ulcerative colitis

Data availability: Data are available on reasonable request.

Synopsis

Appendectomy suppresses a major site of T-cell priming in the colon resulting in a reduced colitis-associated colorectal cancer immunosurveillance. The fundamental mechanism identified emphasizes that precautions will be necessary if appendectomy becomes an accepted treatment of ulcerative colitis.

Abstract

Background & Aims: While appendectomy may reduce colorectal inflammation in patients with ulcerative colitis (UC), this surgical procedure has been suggested to be associated with an increased risk of colitis-associated cancer (CAC). Our aim was to explore the mechanism underlying the appendectomy-associated increased risk of CAC.

Methods: Five-week-old male BALB/c mice underwent appendectomy, appendicitis induction or sham laparotomy. They were then exposed to azoxymethane/dextran sodium sulfate (AOM/DSS) to induce CAC. Mice were sacrificed 12 weeks later, and colons were taken for pathological analysis and immunohistochemistry (CD3 and CD8 staining). Human colonic tumors from 21 patients with UC who underwent surgical resection for CAC were immunophenotyped and stratified according to the appendectomy status.

Results: While appendectomy significantly reduced colitis severity and increased CAC number, appendicitis induction without appendectomy led to opposite results. Intra-tumor CD3+ and CD8+ T-cell densities were lower after appendectomy and higher after appendicitis induction compared to the sham laparotomy group. Blocking lymphocyte trafficking to the colon with the anti-α4β7 integrin antibody or a sphingosine-1-phosphate receptor agonist suppressed the inducing effect of the appendectomy on tumors' number and on CD3+/CD8+ intra-tumoral density. CD8+ or CD3+ T cells isolated from inflammatory neo-appendix and intravenously injected into AOM/DSS-treated recipient mice increased CD3+/CD8+ T-cell tumor infiltration and decreased tumor number. In UC patients with a history of appendectomy, intra-tumor CD3+ and CD8+ T-cell densities were decreased compared to UC patients without history of appendectomy.

Conclusions: In UC, appendectomy could suppress a major site of T-cell priming resulting in a less efficient CAC immunosurveillance.

Keywords: Appendectomy; Appendicitis; Ulcerative Colitis; Inflammatory Bowel Disease.

Introduction

In 1871, Charles Darwin has described the appendix as a rudimentary and useless vestige, that appeared as a consequence of a progressive shrinking of the cecum due to diet changes in our distant ancestors [1]. This historical conception has been refuted by a modern analysis of the evolutive history showing that the appendix has been positively selected among mammals for at least 80 million years and has made multiple independent appearances without any association with diet changes or cecum shrinking [2, 3], pointing out a potential benefit of this structure, the function of which is still almost uncertain [4].

An important question has been raised regarding whether removing the normal appendix is safe or not over time. This question is especially important given the recent improvements in the treatment of ulcerative colitis (UC). The incidence of this inflammatory bowel disease (IBD) can reach up to 465 cases per 100,000 inhabitants in developed countries [5] and it is characterized by chronic inflammation of the rectum and colon. Additionally, the risk of developing colorectal cancer (CRC), referred to as colitis-associated cancer (CAC), is increased in UC patients [6]. A history of appendicitis is rare in UC patients and a reduced incidence of UC has been observed in families with a history of appendicitis [7]. This suggests either a protective effect of appendectomy for colitis [8] or that appendicitis and UC involve alternative inflammatory responses [9].

Interestingly, a history of appendectomy in subjects younger than 20-year-old reduces the risk of developing UC in the general population, only in case of actual appendix inflammation [8, 10]. In contradiction with these findings, the protective effect of preemptive appendectomy without appendicitis has been investigated as a potential therapy for refractory UC and a clinical improvement has been shown in up to 50% of patients [11]. The possible effect of appendectomy on UC clinical outcomes could be a promising therapeutic option [12, 13] but

so far, evidence is lacking to use elective appendectomy as a routine therapeutic procedure in UC.

Data on the use of appendectomy as a therapeutic option are contradictory. While some studies have shown a decreased colectomy rate after appendectomy in UC patients, especially when performed after the onset of the disease [14], other studies have suggested an increased risk of CAC after appendectomy and no significant change in colectomy rate despite a significant reduction in colorectal inflammation [15, 16]. Since it is commonly accepted that CAC is related to colitis severity and extent [17], this last finding is counterintuitive and the mechanisms of this paradoxical effect remain to be investigated.

We have previously shown that appendectomy performed in a mouse model of UC led to a spontaneous onset of colonic tumors [16]. To further decipher the underlying mechanisms involved in appendectomy-induced CAC tumorigenesis, we investigated appendectomy consequences on immunosurveillance and lymphocyte trafficking in a mouse model of CAC. We then confirmed these results in colorectal tumors from patients with UC.

Results

Appendectomy increases tumorigenesis of CAC without worsening colitis

We first investigated the impact of appendectomy on CAC development in the AOM/DSS model. This AOM/DSS murine model aims to induce colon tumors in the setting of chronic colitis *via* the administration of azoxymethane (AOM), a carcinogenic agent, and of dextran sodium sulfate (DSS), a colitogenic agent, as shown in figure 1A. A significantly increased number of colorectal tumors was macroscopically observed in the appendectomy group (24.5 [20.0-31.8] tumors) compared to the control group (sham laparotomy) (15.0 [11.8-22.3] tumors, P=0.0028, figure 1B-C). This increase was confirmed microscopically (13.5 [12.3-19.8] tumors *versus* 9.0 [7.5-10.3] tumors per slide, P <0.0001, figure 1D-E).

As chronic inflammation is the primary cause of CAC, we first explored the impact of appendectomy on chronic colitis severity after the third DSS cycle without initial injection of AOM according to the "DSS-only protocol". This "DSS-only protocol" consisted in colitis evaluation at the end of the third cycle of DSS independently of CAC in order to assess the effect of appendectomy only on chronic colitis (figure 1F). Body weight changes during each DSS cycle and length of the colon did not significantly differ between the appendectomy and control groups (figure 1G-H). However, the histological assessment revealed that appendectomy significantly reduced the extent of colitis compared to controls (P=0.0453, figure 1I), suggesting that appendectomy could moderately decrease the severity of chronic inflammation.

Reduced colonic inflammation following appendectomy has also been reported in patients with UC [11]. However, it is classically admitted that the risk of developing CAC correlates with colitis severity in UC while we observed a concomitant paradoxical increase in the number of colonic tumors. To explore this counterintuitive result, mice were exposed to the AOM/DSS protocol at four different DSS concentrations from 0.5% to 2.0%. We found a positive

correlation between the DSS concentration and colitis severity (figure 2A), and the number of colonic tumors (figure 2B-C), confirming a role of inflammation in tumorigenesis and thus suggesting that appendectomy increased tumorigenesis through a mechanism other than inflammation.

To assess whether appendectomy induced specific tumorigenic pathways, we profiled the molecular landscape of tumors from appendectomized and control mice. The comparative transcriptome analysis of tumors revealed a similar gene expression profile between both groups. Among the 23,517 RNA transcripts analyzed, only 21 (0.1%) were differentially expressed due to appendectomy (figure 3A). In addition, tumor proliferation assessed by immunohistochemistry staining of PCNA was similar in both groups (figure 3B). Thus, no specific tumor molecular pattern was identified in appendectomized mice.

The appendix may be instrumental in maintaining the intestinal microbiome [18] and gut dysbiosis could be a relevant hypothesis to explain the increased tumorigenesis.

The non-spore-forming Gram-negative bacteria, *Fusobacterium nucleatum*, have been associated with both acute appendicitis [19], mild colitis in UC [20], and more severe forms of sporadic CRC in humans [21]. To date, the specific consequences of this bacteria on the CAC are unknown in human, nevertheless a recent published study in mice reported that this bacteria may accelerate the progression of CAC in the AOM-DSS model [22]. Thus, we assessed the intra-tumor infiltration of *Fusobacterium nucleatum* by qPCR in individual tumors. *Fusobacterium nucleatum* was detected in 1 out of 7 and in 1 out of 5 mice (figure 4A and 4B) in the appendectomy and control groups, respectively, indicating that *Fusobacterium nucleatum* was not directly involved in the tumorigenic mechanisms.

We further investigated the overall composition of the fecal microbiota one week after surgery and before DSS treatment. This time point was selected to identify the specific effects of appendectomy, avoiding the indirect effects of inflammation [23] and tumorigenesis on the

microbiota composition. 16s rRNA sequencing of the fecal microbiota revealed a similar abundance of the 7 most represented bacterial phyla between control and appendectomized mice (figure 3C). Both alpha diversity, assessed as the observed richness (Chao1) and diversity (Shannon), (figure 3D) and beta diversity, measured based on the Bray-Curtis or Jaccard indexes, did not significantly differ between both groups (figure 3E-F). LEfSe (Linear discriminant analysis Effect Size) analysis on the fecal microbiota composition did not shown any differences between the two groups, except for the genus *Roseburia* (figure 3G). All in one, our microbiota analysis suggests, in the limits of our explorations, a comparable profile of the fecal microbiota 1 week after the surgery between the appendectomy and the control groups.

Appendectomy reduces intra-tumor T-cell infiltration

To determine the importance of the immunological function of the cecal patch (the murine equivalent of the lymphoid structures of the human appendix) in colitis-associated tumorigenesis, we focused on the anti-tumor immunity driven by CD3+ and CD8+ T cells [24]. Immunohistochemistry showed a significant decrease in CD3+ and CD8+ T-cell tumor infiltration after appendectomy (P=0.0001 figure 5A-B and P=0.031 figure 5C-D, respectively). We further characterized T cells infiltrating CAC by multiparameter flow cytometry (figure 5E-N). The proportion of intra-tumor memory T cells (CD3+ and $CD44^{high}$ cells among CD3+ cells) (figure 5E) was not affected by appendectomy (P=0.5382) even in the subgroups of CD4+ T cells (P=0.4059) (figure 5H) and CD8+ T cells (P=0.3203) (figure 5K). Among memory T cells (CD3+ and $CD44^{high}$ cells), the ratio between effector ($CD62L^{low}$) and central ($CD62L^{high}$) memory T cells was significantly decreased after appendectomy (P=0.0398) (figures 5F and 5N). Accordingly, it is noteworthy that the *SELL* mRNA encoding CD62L was overexpressed in tumors after appendectomy (see figure 3A). Percentages of $PD1^{high}$ T-cells among CD3+ T cells and CD8+ T cells were reduced in the appendectomy group, suggesting a lower proportion

of intra-tumor exhausted T cells (figure 5G and 5M, respectively). However, the functional evaluation of intra-tumor T cells stimulated with PMA-ionomycin did not confirm this hypothesis (figure 5O).

Of note, at the DSS treatment endpoint (DSS-only protocol), CD3+ and CD8+ T-cell densities in the lamina propria were significantly reduced after appendectomy (figure 6A-D), in line with the observation of less severe colitis. In contrast, one week after surgery without AOM/DSS treatment (Surgery-only protocol), CD3+ and CD8+ T-cell densities in the lamina propria were low and did not differ between groups (figure 6E-H). The number of isolated lymphoid follicles in the colon was also unchanged (figure 6I-J). These findings suggested that the immunological impact of appendectomy was mainly observed in case of colitis.

Overall, in tumors from appendectomized mice, $CD8^+$ T-cell infiltration was decreased and the cell phenotype was switched from effector memory T cells to central memory T cells. This finding suggested that the increased CAC development after appendectomy was associated with decreased immune induction and surveillance.

Inhibiting lymphocyte trafficking mitigates the pro-tumor effect of appendectomy

As a key inducer site, the appendix could orchestrate anti-tumor immunity in the colon in the context of chronic inflammation and antigenic stimulation. To test this hypothesis, intestinal homing of lymphocytes from the bloodstream to the gut was reduced with an anti-α4β7 integrin antibody in the one hand and lymphocyte egress from mesenteric lymph nodes and the appendix was inhibited with FTY720 on the other hand. Both blockades were supposed to mimic in part the pro-tumor effect of appendectomy although their own mechanism of action on lymphocyte trafficking into the appendix is unknown.

As expected, anti-α4β7 integrin treatment eliminated the macroscopic and microscopic differences in tumor number between the AOM/DSS appendectomy + anti-α4β7 integrin and

anti-α4β7 integrin only groups (figure 7A-B). Furthermore, anti-α4β7 integrin treatment reduced intra-tumor CD3+ and CD8+ T-cell densities that became similar between appendectomy + anti-α4β7 integrin and anti-α4β7 integrin only groups (figure 7C-D). FTY720 treatment led to identical findings (figure 7E-H). Together, these experiments supported a defect of protective T-cell trafficking to the gut in the mechanism of appendectomy-associated tumorigenesis.

Appendicitis protects against CAC and induces intra-tumor T-cell infiltration

We then assumed that appendicitis could have effects on tumorigenesis opposite to those induced by appendectomy, through the activation of immune surveillance and lymphocytes. Therefore, we explored the potential benefit of inducing neo-appendicitis (figure 8A), on anti-tumor immune protection. As part of the AOM/DSS protocol, significant decreases in macroscopic (P=0.0075) and microscopic (P=0.0035) tumor numbers were detected in the appendicitis group compared to the control group (figure 8B-C). As expected, CD3+ and CD8+ T-cell infiltration was significantly increased in CAC after appendicitis (figure 8D-E). Of note as part of the DSS-only protocol, no significant difference in body weight change after each DSS cycle was observed between the appendicitis and control groups (figure 8F). However, the pathological analysis showed that appendicitis increased colitis extent throughout the colon compared to the control group (P=0.0453, figure 8G). Thus, appendicular inflammation could worsen colitis and induce a phenotype opposite to that observed after appendectomy.

Systemic injection of CD3+ or CD8+ T cells activated by appendicitis protects against CAC and induces intra-tumor T-cell infiltration

To further validate the role of circulating T cells, neo-appendicitis was surgically induced in 27 donor mice and appendicular cells were isolated and purified one week later. T-cell depleted

immune cells (CD45+ CD3- cells) or purified CD3+ T cells or CD8+ T cells were injected into the retro-orbital venous sinus of recipient mice that were further treated with AOM/DSS. Mice injected with CD3+ or CD8+ T cells showed a significant reduction in the number of colonic tumors compared to mice injected with CD45+ CD3- cells (figure 9A-B). A parallel increase in intra-tumor CD3+ and CD8+ T-cell densities was observed (figure 9C-D). No difference in tumor number or intra-tumor T-cell infiltration was noted between mice that received a CD3+ or CD8+ T-cell systemic injection.

The reduced intra-tumor CD3+ and CD8+ T-cell infiltration observed in mice after appendectomy is confirmed in CAC samples from UC patients

To confirm our results obtained in mice in humans, we analyzed colonic tumors from 21 consecutive UC patients who underwent colorectal resection for CAC between January 2006 and December 2017. Five patients (24%) had a history of appendectomy and 16 patients (76%) did not have any history of appendectomy. Clinical and oncological characteristics are summarized in table 1.

More than one CAC (synchronous tumors) was found in the surgical specimen in one patient with a history of appendectomy (2 tumors) and in one patient without history of appendectomy (3 tumors). Thus, we assessed by immunohistochemistry 6 tumors in the appendectomy group and 18 tumors in the control group. The analysis of intra-tumor T cells confirmed that patients with a history of appendectomy had significantly lower CD3+ and CD8+ T-cell densities compared to patients without history of appendectomy (respectively P=0.0044, figure 10A-B and P=0.0472, figure 10C-D).

Discussion

Our results showed that appendectomy was associated with a reduced CD3+ and CD8+ T-cell infiltration in CAC in both mice and humans. In animal models, appendectomy increased colitis-associated tumorigenesis by preventing T-cell trafficking and the subsequent decrease in immune surveillance of cancer. As a mirror image, neo-appendicitis reinforced the protection against CAC through an increase in CD3+ and CD8+ T-cell immunosurveillance. The appendix thus appeared as a major inducer site for T-cell priming of colonic T lymphocytes and could also prime intra-tumor T cells in the context of CAC.

The negative impact of low intra-tumor CD3+ and CD8+ T-cell densities on the prognosis of sporadic CRC is well established [25]. The immunoscore based on CD3+ and CD8+ T-cell densities in sporadic colorectal tumors and in their invasive margins is a powerful prognostic marker for tumor evolution [24]. Intra-tumor CD3+ and CD8+ T-cell densities in CAC have been reported in two contradictory studies. Michael-Robinson *et al*. have highlighted higher densities in CAC [26], whereas Seung Soh *et al.* have observed lower densities [27]. Whatever, low intra-tumor CD3+ and CD8+ density was associated with a poorer tumor prognosis in CAC as in sporadic CRC [27]. Here, we demonstrate in a mouse model of CAC that lower densities of these cell populations were associated with a higher number of tumors, suggesting a protective role of intra-tumor CD3+ and CD8+ T cells. Interestingly, both the transcriptome analysis and the proliferation of CAC were similar between control and appendectomy groups suggesting that the protective role of T-cell immunity conferred by the presence of the appendix might be mainly involved in the protection against tumor initiation rather than tumor progression.

After appendectomy, the number of CD3+ and CD8+ T cells was reduced in both human and mouse with CAC, raising the question of the role of the appendix in cancer immunosurveillance. However, the limited number of CAC analyzed in human did not allow

to go further in the exploration of the data with a statistical analysis adjusted on the confounding factors. Noteworthy, the lower intra-tumor CD3+ and CD8+ T-cell densities in mice were associated with a change in T-cell phenotype characterized by a reduced $CD62L^{low}/CD62L^{high}$ ratio among memory T cells (CD3+ and $CD44^{high}$). $CD3+/CD44^{high}/CD62L^{low}$ and $CD3+/CD44^{high}/CD62L^{high}$ cells are effector (Tem-cell) and central (Tcm-cell) memory T cells, respectively [28]. The proportion of Tem-cells and Tcm-cells generated after antigen presentation to naïve T cells is not constant and depends on the intensity of the antigen exposure: the differentiation into Tem-cells requires a strong antigen exposure while it is the opposite for Tcm-cells [29, 30]. The appendix is a lymphoid structure where intestinal microbiota and environmental antigens are sampled and presented to the immune system [31]. The appendix is thus a major priming site in the colon, able to locally induce Tem-cells and its surgical resection is likely to reduce T-cell education with a significantly decreased Tem-cell/Tcm-cell ratio.

Appendectomy is also associated with a decreased expression of PD1 by T cells in tumors. Intra-tumor exhausted T cells are characterized by a high PD1 expression and an impaired effector function [32]. Indeed, the capacity of these exhausted T cells to proliferate and produce effector cytokines is reduced. Here, we found a low proportion of $PD1^{high}$ T cells after appendectomy but similar cytokine levels between the appendectomy and control groups. This finding suggests that $PD1^{high}$ T cells are not exhausted T cells. Beswick et *al.* have shown that PD1 is upregulated in inflamed colonic mucosa [33]. In line with our results, Yassin et *al.* [34] have shown a progressive increase in PD1 expression over time in the mucosal T-cell subset using the AOM/DSS model. Further CAC treatment with antibodies directed against PD1 has failed to reactivate $PD1^{high}$ T cells directed against the tumors [34]. Recently, we have shown that using anti-PD1 treatment in the AOM/DSS model led to an increased tumor proliferation

[35]. Therefore, PD1 upregulation could reflect previous colonic inflammation rather than an exhausting state of intra-tumor T cells.

CAC is a consequence of DSS-induced colonic inflammation. In the DSS-only model of colitis, colitis extent was reduced and the CD3+ and CD8+ T-cell densities in the lamina propria were significantly reduced after appendectomy. These findings are consistent with a loss of T-cell priming in the appendix even if other mechanisms could be involved [36-38].

T-cell trafficking blockade with an anti-α4β7 integrin antibody or FTY720 mimicked the effect of the appendectomy on the median number of tumors in the AOM/DSS model of CAC. The loss of differences in tumor number and the reduced intra-tumor CD3+/CD8+ T-cell densities between the appendectomy and appendectomy after trafficking blockade suggested that the effect of appendectomy could be mediated by lymphocyte recirculation towards the colonic lamina propria and tumors. Finally, a protection against CAC induced by intra-tumor CD3+/CD8+ T cells primed in the appendix was strongly supported by the T-cell transfer experiments. Indeed, intravenous injection of intra-appendicular CD3+/CD8+ T cells obtained from donor mice in which neo-appendicitis was induced increased tumor infiltration by T cells and limited tumor number in recipient mice. This demonstrates that CD8+ T cells can acquire an efficient immunity against tumorigenesis through an initial priming in the appendix that does not imply exposition to a specific tumor antigen.

Importantly, our results do not suggest that a systematic increased risk of CAC would be inherent to all immunosuppressive or immunomodulatory treatments given to patients with UC. Two parameters should be considered to assess this risk, which are the treatment efficiency on the colonic inflammation and the mechanism of action of the treatment. As these two parameters differ between each treatment, our results regarding the impact of appendectomy on the risk of CAC can in no way be extrapolated to the impact of other treatments. To warrant

this point, a significant lower risk of developing a CAC in IBD patients treated by immunosuppressive therapy such as thiopurines [39] or by anti-TNFα [40] has been reported.

A higher risk of CAC despite a decrease of UC severity is not only reported in the specific context of the appendectomy but also in patients with UC with a concomitant primary sclerosing cholangitis (PSC) [41, 42]. As we know up to now, the toxicity of bile acids is suspected of being implicated in the increased risk of CAC in patients with PSC. It is assumed that liver cholestasis observed during PSC would decrease the absorption of bile acids in the digestive tract [43] leading to an elevation of bile acid concentration in the colon, and specifically of the secondary bile acids which are known to be carcinogenic for the colon [44]. Thus, despite a similar phenotype between patients with UC with a concomitant PSC and patients with UC with a history of appendectomy, the mechanism involved seems to be totally different.

If the appendix plays a crucial role in CAC, why is the oncological immunosurveillance provided by CD8+ T cells primed in the appendix not effective in sporadic CRC? In industrialized countries, about 10% of the population will undergo appendectomy during their life [45]. Despite a high incidence of sporadic CRC, a history of appendectomy is not known as a risk factor [46]. However, in most cases, appendectomy is performed for acute appendicitis. Indeed, a Taiwanese national cohort study has confirmed that a history of appendectomy for appendicitis was not associated with a risk of cancer (hazard ratio (HR): 1.02, 95%CI [0.90-1.16]) but a history of incidental appendectomy without appendicitis was significantly associated with a risk of sporadic CRC (HR: 2.90, 95%CI [2.24-3.75]) [47]. This finding suggests that the appendix could also play a role in sporadic CRC.

In conclusion, using a mouse model of CAC, we showed that appendectomy induced a pro-tumorigenic effect mediated by intra-tumor T-cell infiltration. Blocking cell egress from the appendix or T-cell homing to the colon mimicked the appendectomy-associated phenotype

whereas re-injecting appendix-primed T cells increased intra-tumor T-cell infiltration. In UC patients with CAC, appendectomy was associated with a decreased intra-tumor T-cell infiltration. The fundamental mechanism identified in this study emphasizes that precautions will be necessary if appendectomy becomes an accepted therapeutic option for the treatment of refractory UC.

Methods

Animal models

All experimental procedures were approved by our local Animal Ethics Committee and the French Ministry of Research in accordance with the European legislation (APAFIS n° 14004-2018030914101923v5 and 24604-2020030518127896v3).

Five-week-old male BALB/c mice were purchased from Charles River and housed in ventilated cages with free access to water and food under controlled temperature (22 ± 2°C) and humidity (50 ± 10%). Mice were randomly assigned to experimental and control groups and the azoxymethane/dextran sodium sulfate (AOM/DSS) model of CAC was induced [48]. Mice were injected intraperitoneally with AOM (10 mg/kg of body weight; Sigma-Aldrich) at day 0. One week later, mice were treated with DSS (MW=36,000–50,000; MP Biomedicals) in sterile drinking water according to the following sequence: 1.5% DSS for 7 days (first DSS cycle), sterile drinking water for 7 days, 1.5% DSS for 7 days (second cycle), sterile drinking water for 14 days and 1.5% DSS for 4 days (third cycle). Between the end of the third DSS cycle and sacrifice, mice had free access to DSS-free drinking water. Mice were weighed once a week all along the AOM/DSS protocol and the clinical severity of colitis was assessed during each DSS cycle based on the percentage of weight change. Mice were sacrificed 12 weeks after AOM injection. To induce chronic colitis without CAC, mice underwent 3 DSS cycles without prior injection of AOM (DSS-only protocol). Colonic specimens were collected for blinded histological evaluation and further biological and biochemical analyzes.

Surgical procedures

Surgery was performed under general anesthesia (intraperitoneal injection of buprenorphine at 0.1 mg/kg and inhalation of 3% isoflurane during the induction, and then 1.5% isoflurane during the procedure). Three different surgical procedures were performed: appendectomy,

appendicitis induction and sham laparotomy (thereafter referred to as “control”). All mice underwent a single surgical procedure. After initiation of anesthesia, the skin was shaved and prepped with 70% ethanol. In the left iliac fossa, 1-cm paramedian laparotomy was performed, and the cecum was externalized from the peritoneal cavity. The cecal patch was identified as a 2-mm white ovoid structure on the antimesenteric side of the cecum. The appendectomy procedure consisted in the resection of the cecal patch. This structure is a major lymphoid structure in the colon of mice, located at the end of the cecum, and corresponds to the human appendix lymphoid structure [16, 49]. Bacterial translocation occurs in the murine cecal patch via microfold (M) cells [50] as observed in the human appendix [31] recapitulating its immune function. Nevertheless, the cecal patch is a flat surface that does not have the cul-de-sac shape of the human appendix, thus does not reproducing the microbiota sanctuary function. To perform the resection of the cecal patch, this structure was suctioned with a 1-ml plastic syringe, ligated at its base with Corolene® 8/0 thread and resected. Then, the cecum was reintegrated into the abdomen and the abdominal wall was closed with two layers (muscles and skin) of Filapeau® 6/0 continuous sutures. To induce experimental appendicitis, the cecal patch was ligated at its base but not resected, leading to local inflammation that resolved spontaneously without any antibiotics or secondary appendectomy. For the sham procedure, the cecum was externalized and reintegrated into the abdomen without any ligation of the cecal patch (control group). Buprenorphine (0.1 mg/kg) could be administered postoperatively in case of apparent pain but no other treatments such as anti-inflammatory drugs or antibiotics were administered. As part of the AOM/DSS protocol, surgery was performed at the same time as the AOM injection, i.e., 1 week before starting the first DSS cycle. AOM was injected into the peritoneal cavity at the end of the procedure, after abdomen closure. Similarly, as part of the DSS-only protocol, surgery was performed 1 week before starting the first DSS cycle. A third protocol called “surgery-only” was used to assess the effect of surgery in the absence of colitis and CAC.

As part of this protocol, mice underwent surgery (appendectomy, appendicitis or sham laparotomy) and were sacrificed 1 week later without any administration of AOM or DSS.

Human samples

From January 2006 to December 2017, all UC patients (n=21) who underwent surgical resection for CAC in our institution (Beaujon hospital, Clichy, France) were included. Patients with Crohn's disease or unclassified IBD or with dysplastic lesions only were excluded. Patients' clinical characteristics were retrospectively collected. Paraffin-embedded CAC samples were collected for pathological analysis and immunohistochemistry. Any history of appendectomy was obtained from the pathology report of (sub-)total colectomy or coloproctectomy describing the presence or the absence of an appendix on the surgical specimen. Paraffin-embedded blocks with colorectal tumor fragments were collected for immunohistochemistry.

This study was approved by our local Ethics Committee and the French Ministry of Research (n° 12.739) in accordance with the European legislation.

Pathology

After sacrifice of mice, the entire colon was removed, opened in the longitudinal axis and macroscopically-visible tumors were counted. Then, swiss rolls of colons were fixed for 24h in 10% formalin and embedded in paraffin to observe the full-length organ. Paraffin-embedded sections (5 µm) were deparaffinized, stained with H&E reagent and the number of microscopically-visible tumors was determined. The colitis severity was assessed by the histological extent of colitis [51]. Tissue sections from mice that underwent the DSS-only protocol were digitized (Scanscope AT turbo, Leica). Histological lesions of colitis were

delineated with Aperio ImageScope software to calculate the percentage of inflamed colonic epithelium surface within the entire colonic epithelium for each mouse.

Immunohistochemistry

Paraffin-embedded colonic sections (5 µm) from each mouse were prepared for immunohistochemistry using antibodies directed against CD3 (ab16669, Abcam, 1/150 dilution) and CD8 (ab209775, Abcam, 1/1,000 dilution). Tissue slides from AOM/DSS-treated mice were also stained with antibodies directed against PCNA (Sc-56, Biotechnology, 1/100 dilution) to assess tumor cell proliferation. Tumor sections from human samples were analyzed by immunohistochemistry using antibodies directed against CD3 (A0452, Dako, 1/50 dilution) and CD8 (M7103, Dako, 1/50 dilution). Immunostained slides were digitized with Scanscope AT turbo, Leica. Using Aperio ImageScope software, human and mouse tumors were delineated. Tumor surfaces and the number of cells stained with the specific antibodies were automatically quantified. The median intra-tumor CD3+ and CD8+ T-cell densities were then calculated. This method was thus observer-independent. The lamina propria was also delineated on slides from mice that underwent the Surgery-only and DSS-only protocols. The surface and number of cells stained with the specific antibodies were quantified to assess the median CD3+ and CD8+ T-cell densities.

Isolation of intra-tumor T cells

Colonic tumors obtained at the end of the AOM/DSS protocol were collected, taking care to not remove the adjacent healthy colon. All tumors from the same colon were pooled in 10 mL of RPMI 1640 medium with GlutaMAX (61870-010, Gibco) supplemented with 10 mg of type IV Collagenase (LS004188 Serlabo), 0.5% of fetal bovine serum (FBS) and 10 mg of DNase (DN25-100MG Sigma). Fresh tumors were transferred to gentleMACS tubes (130-096-334,

Miltenyi). Digestion was performed with gentleMACS Dissociator for 36 minutes at 37°C and with subsequent centrifugation at 930 rpm (37C_m_LIDK_1 program). After collagenase digestion and mechanical disruption, a single-cell suspension was obtained after filtration with 100-µm and then 40-µm cell strainers and washed twice with RPMI. To increase T-cell concentration, intra-tumor T cells were selected using Mouse CD90.2 MicroBeads (130-121-278, Miltenyi) according to the manufacturer's instructions. Magnetic separation was performed with the MultiMACs Separator Plus (130-098-637, Miltenyi).

Flow cytometry

Cell suspensions were Fc-blocked (FcR Blocking mouse, 130-092-575 Miltenyi) and dead cells were stained with LIVE/DEAD Fixable Aqua Dead Cell Stain Kit-AmCyan (L34957, Thermofisher). Then, cells were incubated for 20 minutes at 4°C in the dark with a cocktail of antibodies directed against CD3 (APC-Vio770, 130-119-793 Miltenyi), CD4 (FITC, 130-118-692, Miltenyi), CD8 (PE-Vio770, 130-119-123, Miltenyi), CD62L (APC, 130-112-837, Miltenyi), CD44 (PE, 130-118-694, Miltenyi) and PD1 (PE-CF594, 562523 BD). Samples were washed twice with PBS (phosphate buffered saline). Samples were acquired using LSRFortessa (BD) and analyzed with FlowJo v10.

T-cell stimulation and cytokine measurement by ELISA

For each mouse, 100,000 intra-tumor T cells were transferred to 96-well plates with 200 µL of cell culture medium in the presence or in the absence of a stimulation cocktail of PMA and ionomycin (00-4970-93; 1/500 dilution; Thermofisher). Cell culture medium included RPMI 1640 with GlutaMAX, 10% of FBS and 1% of antibiotic-antimycotic (15240096, Thermofisher). After 16 hours in a humidified 37°C incubator with 5% CO_2, supernatants were collected and stored at -20°C for cytokine assay. Concentrations of TNF-α and INF-γ were

measured by ELISA according to the manufacturer's instructions (respectively 88-7324-22 and 88-7314-22; Thermofisher). Detection ranges were 8-1,000 pg/mL for TNF-α and 15-2,000 pg/mL for INF-γ.

Transcriptome analyzes

Total RNAs were extracted from fresh colonic tumors using the RNAble Kit (Eurobio) and quantified with a nanodrop-1000 spectrophotometer (Thermofisher). Microarray processing was performed by a genomic platform (genom'IC, Cochin Institute, Paris, France). After validation of the RNA quality with the Bioanalyzer 2100 (using the Agilent RNA6000 nano chip kit), 100 ng of total RNAs were reverse transcribed using the GeneChip® WT Plus Reagent Kit (Thermofisher). Briefly, the resulting double-strand cDNA was used for *in vitro* transcription with T7 RNA polymerase (all these steps are included in the WT cDNA synthesis and amplification kit from Thermofisher). After purification according to Thermofisher protocol, 5.5 µg of Sens Target DNA were fragmented, biotin labelled and controlled using the Bioanalyzer 2100. cDNAs were then hybridized to GeneChip® MouseGene2.0ST (Affymetrix) at 45°C for 17 hours, and the chips were washed on the FS450 fluidics station (Affymetrix) and scanned using the GCS3000 7G. Scanned images were then analyzed with Expression Console software (Affymetrix) to obtain raw data (CEL files) and metrics for Quality Controls. No apparent outlier value was detected. CEL files were normalized by Robust Multi-array Averaging (RMA) in the Bioconductor R with the Brain Array custom CDF vs 23. Statistical analyzes were performed with Partek® GS. A t-test was used to explore differences in expressed genes between the appendectomy and control groups. Only genes with p-values <0.05 and expression fold-changes >1.5 were considered differentially expressed between both groups.

Fecal microbiota characterization

Mouse fecal samples were collected one week after surgery and frozen at -80°C. DNA was extracted using the QIAamp Fast DNA Stool Mini Kit (51604, Qiagen). A mechanical lysis with FastPrep (MP Biomedicals) was added to the protocol before thermal lysis. DNA concentration was measured using the Qubit dsDNA High Sensitivity Assay Kit (Q32851, Thermofisher) and adjusted for each sample to 5 ng/µL. 16S rRNA genes were amplified by PCR with universal primers amplifying the V4 variable region (515F: GTGCCAGCMGCCGCGGTAA and 806R: GGACTACHVGGGTWTCTAAT) [52]. Barcodes and Illumina sequencing adapters were attached using the Nextera XT Index Kit (Illumina). Amplicons were purified using Agencourt AMPure (Beckman Coulter), quantified by qPCR using the KAPA Library Quantification Kit (Roche), pooled in equimolar concentration and diluted to 5.5 pM for sequencing. Sequencing was performed on the Illumina Miseq (600 cycles, 2x300 bp, paired sequences). Sequencing data was processed in R (version 4.1.2) using the DADA2 pipeline [53]. Quality profiles of the reads were analysed, filtered and trimmed. Forward and reverse denoised reads were merged together. The amplicon sequence variant (ASV) table was constructed with the full denoised sequences. After the removal of chimeras (method="consensus"), taxonomy was assigned from 16S rRNA database Silva 138.1 [54]. Data obtained were assembled and converted into a phyloseq object [55]. Abundance, alpha and beta diversity measurements were performed with the Shiny Migale script (https://shiny.migale.inrae.fr/app/easy16S/). Alpha diversity indices (Chao1 and Shannon) were calculated for each sample and compared between the appendectomy and control groups using an ANOVA analysis. A principal coordinates analysis based on the distance matrix of the beta diversity indices (Bray Curtis and Jaccard) was used to visualize differences in microbial composition between groups. Significance was assessed using a PERMANOVA (Permutational

Multivariate Analysis of Variance Using Distance Matrices) test. A P-value <0.05 was considered significant.

A *LEfSe* (Linear discriminant analysis Effect Size) analysis was conducted to assess the bacterial taxa enriched in the feces of the appendectomy and of the control groups [56]. To do so, first we added a refseq slot to the phyloseq object (*Microbiomeutilities* package) , then LefSe analysis was run based on p-value <0.05 and on a LDA >4. Results were plotted in a cladogram.

Quantitative PCR for the detection of Fusobacterium nucleatum DNA

Genomic DNA was extracted from fresh colonic tumors using the DNeasy Blood and Tissue kit (Qiagen). DNA was quantified using a Qubit 3.0 Fluorometer (Thermo Fisher Scientific). Real-time qPCR was performed with 10 ng or 40 ng of DNA sample, 10 μM of primers and MesaBlue qPCR MasterMix (Eurogentec). *Fusobacterium nucleatum* DNA was detected using the following primers: forward 5'-CCAACCATTACTTTAACTCTACCATGTTCA-3' and reverse 5'-GTTGACTTTACAGAAGGAGATTATGTAAAAATC-3' [57]. To detect the presence of bacterial DNA in samples, a 16S rDNA non-specific PCR was performed using the primers U968 5'-GAACGCGAAGAACCTTAC-3' and L1401 5'-GCGTGTGTACAAGACCC-3' [58]. PCR were carried out using a LightCycler 480 instrument (Roche Diagnostics). Initial denaturation was performed at 95°C for 10 min, followed by 45 cycles consisting of 95°C for 15s and 60°C for 45s. A dissociation step was added, and dissociation curves were analyzed to confirm amplification fidelity. Positive PCR products were sent for sequencing to Eurofins Genomics, and sequences were analyzed through BLAST program (NCBI) to confirm *Fusobacterium nucleatum*-specific amplification.

Blocking lymphocyte trafficking

An anti-integrin α4-β7 antibody and FTY720 (a sphingosine-1-phosphate receptor agonist) were independently used to limit lymphocyte trafficking to the colon. From Day 1 of the first DSS cycle (i.e., 1 week after appendectomy or sham surgery and after the AOM injection) until sacrifice, 125 µg/100µL of InVivoMAb anti-mouse LPAM-1 (integrin α4β7) (BE0034, Bioxcell) or 60 µg/100µL of FTY720 (SML0700, Sigma-Aldrich) were intraperitoneally administered twice a week. Regarding the control group, 100µL of sterile PBS was injected intraperitoneally according to the same chronology as the anti-integrin α4-β7 antibody and FTY720.

Transfers of systemic immune cells isolated from inflamed appendices

One week after appendicitis induction, 27 mice were sacrificed and inflamed appendices were resected and pooled in gentleMACS tubes (130-096-334, Miltenyi) containing 10 mL of RPMI 1640 with GlutaMAX (61870-010, Gibco) supplemented with 10 mg of type IV Collagenase (LS004188 Serlabo), 0.5% of FBS and 10 mg of DNase (DN25-100MG Sigma). Cell digestion and dissociation were performed using the gentleMACS Dissociator for 36 minutes at 37°C with subsequent centrifugation at 930 rpm. After incubation, the single-cell suspension was obtained after filtration with 100-µm and 40-µm cell strainers and washed twice with RPMI. At this step, $2.1x10^8$ living cells were obtained and then divided into two different tubes (tubes A and B). Tube A was used to isolate CD8+ T cells from inflamed appendices using the Mouse CD8a+ T-cell Isolation Kit (130-104-075, Miltenyi). Magnetic separation was performed using the MultiMACs Separator Plus (130-098-637, Miltenyi) according to the manufacturer's instructions. Tube B was used to isolate CD3+ T cells using Mouse CD90.2 MicroBeads (130-121-278, Miltenyi). Appendicular cells depleted in CD3+ T cells were then incubated with Mouse CD45 MicroBeads (130-052-301, Miltenyi). Cell isolation quality was controlled by flow cytometry. Among CD8+ filtered T cells, 87% of living cells were CD8+ and 0.007%

were CD4+. Among CD3+ filtered T cells, 80% of living cells were CD3+, 38% were CD4+ and 39% were CD8+. Among CD45+ cells depleted in CD3+ T cells, 99% of living cells were CD45+ and 92% were CD3-.

CD8+ filtered T cells (CD8+ T-cell injection group), CD3+ filtered T cells (CD3+ T-cell injection group) and CD45+ cells depleted in CD3+ T cells (CD45+CD3- cell injection group) were respectively injected into 8 mice. Each mouse received a standardized injection containing $5x10^5$ living cells in 100 µL of PBS in the retro-orbital venous sinus. At the same time as these systemic cell injections, mice received an intraperitoneal injection of AOM and were then exposed to the 3 DSS cycles according to the AOM/DSS protocol. After sacrifice, 12 weeks after the beginning of the AOM/DSS protocol, tumors were quantified macroscopically and microscopically, and intra-tumor CD3+ and CD8+ T-cell densities were assessed after immunohistochemistry as described above.

Statistics

The sample size of each group of mice was calculated assuming an alpha risk of 0.05, a beta risk of 0.2 and considering a two-sided statistical analysis. This calculation was performed by the free online calculator proposed by Boston Universisty [59]. These sample sizes were checked and validated by our local Animal Ethics Committee and the French Ministry of Research in accordance with the European legislation (APAFIS n°14004-2018030914101923v5 and 24604-2020030518127896v3). Reducing as much as possible the number of animals in accordance with the ethics of animal experimentation was a priority. Quantitative values are expressed as a median [25^{th} percentile-75^{th} percentile]. Comparisons of 2 groups were performed using the Mann-Whitney test with 2-tailed P-value. Comparisons of multiple groups were performed using the Kruskal-Wallis test and, only if the P-value was <0.05, multiple comparisons with *post hoc* tests (Dunn's test) were performed. A P-value <0.05

was considered statistically significant (2-sided tests). Statistical analyzes were performed using Prism v8.2.1 (GraphPad Software).

All authors had access to the study data and had reviewed and approved the final manuscript.

References

[1] Darwin C. The Descent of Man and Selection in Relation to Sex (London: John Murray, 1871), I:27.

[2] Smith HF, Fisher RE, Everett ML, Thomas AD, Bollinger RR, Parker W. Comparative anatomy and phylogenetic distribution of the mammalian cecal appendix. J Evol Biol 2009;22(10):1984-99.

[3] Smith HF, Parker W, Kotzé SH, Laurin M. Morphological evolution of the mammalian cecum and cecal appendix. Comptes Rendus Palevol 2017;16(1):39-57.

[4] Girard-Madoux MJH, Gomez de Aguero M, Ganal-Vonarburg SC, Mooser C, Belz GT, Macpherson AJ, Vivier E. The immunological functions of the Appendix: An example of redundancy? Semin Immunol 2018;36:31-44.

[5] Abou Khalil M, Boutros M, Nedjar H, Morin N, Ghitulescu G, Vasilevsky CA, Gordon P, Rahme E. Incidence Rates and Predictors of Colectomy for Ulcerative Colitis in the Era of Biologics: Results from a Provincial Database. J Gastrointest Surg 2018;22(1):124-32.

[6] Liu X, Goldblum JR, Zhao Z, Landau M, Heald B, Pai R, Lin J. Distinct clinicohistologic features of inflammatory bowel disease-associated colorectal adenocarcinoma: in comparison with sporadic microsatellite-stable and Lynch syndrome-related colorectal adenocarcinoma. Am J Surg Pathol 2012;36(8):1228-33.

[7] Nyboe Andersen N, Gortz S, Frisch M, Jess T. Reduced risk of UC in families affected by appendicitis: a Danish national cohort study. Gut 2017;66(8):1398-402.

[8] Andersson RE, Olaison G, Tysk C, Ekbom A. Appendectomy and protection against ulcerative colitis. N Engl J Med 2001;344(11):808-14.

[9] Beaugerie L, Sokol H. Appendicitis, not appendectomy, is protective against ulcerative colitis, both in the general population and first-degree relatives of patients with IBD. Inflamm Bowel Dis 2010;16(2):356-7.

[10] Frisch M, Pedersen BV, Andersson RE. Appendicitis, mesenteric lymphadenitis, and subsequent risk of ulcerative colitis: cohort studies in Sweden and Denmark. BMJ 2009;338:b716.

[11] Stellingwerf ME, Sahami S, Winter DC, Martin ST, D'Haens GR, Cullen G, Doherty GA, Mulcahy H, Bemelman WA, Buskens CJ. Prospective cohort study of appendicectomy for treatment of therapy-refractory ulcerative colitis. Br J Surg 2019;106(12):1697-704.

[12] Felice C, Armuzzi A. Therapeutic Role of Appendectomy in Ulcerative Colitis: A Tangible Perspective? J Crohns Colitis 2019;13(2):142-3.

[13] Gardenbroek TJ, Pinkney TD, Sahami S, Morton DG, Buskens CJ, Ponsioen CY, Tanis PJ, Lowenberg M, van den Brink GR, Broeders IA, Pullens PH, Seerden T, Boom MJ, Mallant-Hent RC, Pierik RE, Vecht J, Sosef MN, van Nunen AB, van Wagensveld BA, Stokkers PC, Gerhards MF, Jansen JM, Acherman Y, Depla AC, Mannaerts GH, West R, Iqbal T, Pathmakanthan S, Howard R, Magill L, Singh B, Htun Oo Y, Negpodiev D, Dijkgraaf MG, Ram D'Haens G, Bemelman WA. The ACCURE-trial: the effect of appendectomy on the clinical course of ulcerative colitis, a randomised international multicenter trial (NTR2883) and the ACCURE-UK trial: a randomised external pilot trial (ISRCTN56523019). BMC Surg 2015;15:30.

[14] Stellingwerf ME, Bemelman WA, Löwenberg M, Ponsioen CY, D'Haens GR, van Dieren S, Buskens CJ. A nationwide database study on colectomy and colorectal cancer in ulcerative colitis: what is the role of appendectomy? Colorectal Dis 2021;23(1):64-73.

[15] Stellingwerf ME, de Koning MA, Pinkney T, Bemelman WA, D'Haens GR, Buskens CJ. The Risk of Colectomy and Colorectal Cancer After Appendectomy in Patients With Ulcerative Colitis: A Systematic Review and Meta-analysis. J Crohns Colitis 2019;13(3):309-18.

[16] Harnoy Y, Bouhnik Y, Gault N, Maggiori L, Sulpice L, Cazals-Hatem D, Boudjema K, Panis Y, Ogier-Denis E, Treton X. Effect of appendicectomy on colonic inflammation and neoplasia in experimental ulcerative colitis. Br J Surg 2016;103(11):1530-8.

[17] Flores BM, O'Connor A, Moss AC. Impact of mucosal inflammation on risk of colorectal neoplasia in patients with ulcerative colitis: a systematic review and meta-analysis. Gastrointest Endosc 2017;86(6):1006-11 e8.

[18] Randal Bollinger R, Barbas AS, Bush EL, Lin SS, Parker W. Biofilms in the large bowel suggest an apparent function of the human vermiform appendix. J Theor Biol 2007;249(4):826-31.

[19] Swidsinski A, Dorffel Y, Loening-Baucke V, Theissig F, Ruckert JC, Ismail M, Rau WA, Gaschler D, Weizenegger M, Kuhn S, Schilling J, Dorffel WV. Acute appendicitis is characterised by local invasion with Fusobacterium nucleatum/necrophorum. Gut 2011;60(1):34-40.

[20] Tahara T, Shibata T, Kawamura T, Okubo M, Ichikawa Y, Sumi K, Miyata M, Ishizuka T, Nakamura M, Nagasaka M, Nakagawa Y, Ohmiya N, Arisawa T, Hirata I. Fusobacterium detected in colonic biopsy and clinicopathological features of ulcerative colitis in Japan. Dig Dis Sci 2015;60(1):205-10.

[21] Mima K, Nishihara R, Qian ZR, Cao Y, Sukawa Y, Nowak JA, Yang J, Dou R, Masugi Y, Song M, Kostic AD, Giannakis M, Bullman S, Milner DA, Baba H, Giovannucci EL, Garraway LA, Freeman GJ, Dranoff G, Garrett WS, Huttenhower C, Meyerson M, Meyerhardt JA, Chan AT, Fuchs CS, Ogino S. Fusobacterium nucleatum in colorectal carcinoma tissue and patient prognosis. Gut 2016;65(12):1973-80.

[22] Yu MR, Kim HJ, Park HR. Fusobacterium nucleatum Accelerates the Progression of Colitis-Associated Colorectal Cancer by Promoting EMT. Cancers (Basel) 2020;12(10).

[23] Hakansson A, Tormo-Badia N, Baridi A, Xu J, Molin G, Hagslatt ML, Karlsson C, Jeppsson B, Cilio CM, Ahrne S. Immunological alteration and changes of gut microbiota after dextran sulfate sodium (DSS) administration in mice. Clin Exp Med 2015;15(1):107-20.

[24] Pages F, Mlecnik B, Marliot F, Bindea G, Ou FS, Bifulco C, Lugli A, Zlobec I, Rau TT, Berger MD, Nagtegaal ID, Vink-Borger E, Hartmann A, Geppert C, Kolwelter J, Merkel S, Grutzmann R, Van den Eynde M, Jouret-Mourin A, Kartheuser A, Leonard D, Remue C, Wang JY, Bavi P, Roehrl MHA, Ohashi PS, Nguyen LT, Han S, MacGregor HL, Hafezi-Bakhtiari S, Wouters BG, Masucci GV, Andersson EK, Zavadova E, Vocka M, Spacek J, Petruzelka L, Konopasek B, Dundr P, Skalova H, Nemejcova K, Botti G, Tatangelo F, Delrio P, Ciliberto G, Maio M, Laghi L, Grizzi F, Fredriksen T, Buttard B, Angelova M, Vasaturo A, Maby P, Church SE, Angell HK, Lafontaine L, Bruni D, El Sissy C, Haicheur N, Kirilovsky A, Berger A, Lagorce C, Meyers JP, Paustian C, Feng Z, Ballesteros-Merino C, Dijkstra J, van de Water C, van Lent-van Vliet S, Knijn N, Musina AM, Scripcariu DV, Popivanova B, Xu M, Fujita T, Hazama S, Suzuki N, Nagano H, Okuno K, Torigoe T, Sato N, Furuhata T, Takemasa I, Itoh K, Patel PS, Vora HH, Shah B, Patel JB, Rajvik KN, Pandya SJ, Shukla SN, Wang Y, Zhang G, Kawakami Y, Marincola FM, Ascierto PA, Sargent DJ, Fox BA, Galon J. International validation of the consensus Immunoscore for the classification of colon cancer: a prognostic and accuracy study. Lancet 2018;391(10135):2128-39.

[25] Galon J, Costes A, Sanchez-Cabo F, Kirilovsky A, Mlecnik B, Lagorce-Pagès C, Tosolini M, Camus M, Berger A, Wind P, Zinzindohoué F, Bruneval P, Cugnenc PH,

Trajanoski Z, Fridman WH, Pagès F. Type, density, and location of immune cells within human colorectal tumors predict clinical outcome. Science 2006;313(5795):1960-4.

[26] Michael-Robinson JM, Pandeya N, Walsh MD, Biemer-Huttmann AE, Eri RD, Buttenshaw RL, Lincoln D, Clouston AD, Jass JR, Radford-Smith GL. Characterization of tumour-infiltrating lymphocytes and apoptosis in colitis-associated neoplasia: comparison with sporadic colorectal cancer. J Pathol 2006;208(3):381-7.

[27] Soh JS, Jo SI, Lee H, Do EJ, Hwang SW, Park SH, Ye BD, Byeon JS, Yang SK, Kim JH, Yang DH, Kim SY, Myung SJ. Immunoprofiling of Colitis-associated and Sporadic Colorectal Cancer and its Clinical Significance. Sci Rep 2019;9(1):6833.

[28] Sallusto F, Lenig D, Forster R, Lipp M, Lanzavecchia A. Two subsets of memory T lymphocytes with distinct homing potentials and effector functions. Nature 1999;401(6754):708-12.

[29] Wherry EJ, Teichgraber V, Becker TC, Masopust D, Kaech SM, Antia R, von Andrian UH, Ahmed R. Lineage relationship and protective immunity of memory CD8 T cell subsets. Nat Immunol 2003;4(3):225-34.

[30] Marzo AL, Klonowski KD, Le Bon A, Borrow P, Tough DF, Lefrancois L. Initial T cell frequency dictates memory CD8+ T cell lineage commitment. Nat Immunol 2005;6(8):793-9.

[31] Gebbers JO, Laissue JA. Bacterial translocation in the normal human appendix parallels the development of the local immune system. Ann N Y Acad Sci 2004;1029:337-43.

[32] Ahmadzadeh M, Johnson LA, Heemskerk B, Wunderlich JR, Dudley ME, White DE, Rosenberg SA. Tumor antigen-specific CD8 T cells infiltrating the tumor express high levels of PD-1 and are functionally impaired. Blood 2009;114(8):1537-44.

[33] Beswick EJ, Grim C, Singh A, Aguirre JE, Tafoya M, Qiu S, Rogler G, McKee R, Samedi V, Ma TY, Reyes VE, Powell DW, Pinchuk IV. Expression of Programmed Death-Ligand 1 by Human Colonic CD90(+) Stromal Cells Differs Between Ulcerative Colitis and Crohn's Disease and Determines Their Capacity to Suppress Th1 Cells. Front Immunol 2018;9:1125.

[34] Yassin M, Sadowska Z, Djurhuus D, Nielsen B, Tougaard P, Olsen J, Pedersen AE. Upregulation of PD-1 follows tumour development in the AOM/DSS model of inflammation-induced colorectal cancer in mice. Immunology 2019;158(1):35-46.

[35] Collard M, Guedj N, Tourneur-Marsille JA, M., Maggiori L, Hammel P, Treton X, Panis Y, Ogier-Denis E. Immune-checkpoint inhibitor anti-PD1 aggravates colitis-associated colorectal cancer without enhancing intestinal inflammation. Integr Cancer Sci Therap 2020.

[36] Cheluvappa R. Experimental appendicitis and appendectomy modulate the CCL20-CCR6 axis to limit inflammatory colitis pathology. Int J Colorectal Dis 2014;29(10):1181-8.

[37] Cheluvappa R, Luo AS, Grimm MC. Autophagy suppression by appendicitis and appendectomy protects against colitis. Inflamm Bowel Dis 2014;20(5):847-55.

[38] Cheluvappa R, Thomas DG, Selvendran S. The Role of Specific Chemokines in the Amelioration of Colitis by Appendicitis and Appendectomy. Biomolecules 2018;8(3).

[39] Zhu Z, Mei Z, Guo Y, Wang G, Wu T, Cui X, Huang Z, Zhu Y, Wen D, Song J, He H, Xu W, Cui L, Liu C. Reduced Risk of Inflammatory Bowel Disease-associated Colorectal Neoplasia with Use of Thiopurines: a Systematic Review and Meta-analysis. J Crohns Colitis 2018;12(5):546-58.

[40] Alkhayyat M, Abureesh M, Gill A, Khoudari G, Abou Saleh M, Mansoor E, Regueiro M. Lower Rates of Colorectal Cancer in Patients With Inflammatory Bowel Disease Using Anti-TNF Therapy. Inflamm Bowel Dis 2021;27(7):1052-60.

[41] Aranake-Chrisinger J, Dassopoulos T, Yan Y, Nalbantoglu I. Primary sclerosing cholangitis associated colitis: Characterization of clinical, histologic features, and their associations with liver transplantation. World J Gastroenterol 2020;26(28):4126-39.
[42] Zheng HH, Jiang XL. Increased risk of colorectal neoplasia in patients with primary sclerosing cholangitis and inflammatory bowel disease: a meta-analysis of 16 observational studies. Eur J Gastroenterol Hepatol 2016;28(4):383-90.
[43] Hruz P, Zimmermann C, Gutmann H, Degen L, Beuers U, Terracciano L, Drewe J, Beglinger C. Adaptive regulation of the ileal apical sodium dependent bile acid transporter (ASBT) in patients with obstructive cholestasis. Gut 2006;55(3):395-402.
[44] Bernstein C, Holubec H, Bhattacharyya AK, Nguyen H, Payne CM, Zaitlin B, Bernstein H. Carcinogenicity of deoxycholate, a secondary bile acid. Arch Toxicol 2011;85(8):863-71.
[45] Anderson JE, Bickler SW, Chang DC, Talamini MA. Examining a common disease with unknown etiology: trends in epidemiology and surgical management of appendicitis in California, 1995-2009. World J Surg 2012;36(12):2787-94.
[46] Lee J, Choe S, Park JW, Jeong SY, Shin A. The Risk of Colorectal Cancer After Cholecystectomy or Appendectomy: A Population-based Cohort Study in Korea. J Prev Med Public Health 2018;51(6):281-8.
[47] Wu SC, Chen WT, Muo CH, Ke TW, Fang CW, Sung FC. Association between appendectomy and subsequent colorectal cancer development: an Asian population study. PLoS One 2015;10(2):e0118411.
[48] Tanaka T, Kohno H, Suzuki R, Yamada Y, Sugie S, Mori H. A novel inflammation-related mouse colon carcinogenesis model induced by azoxymethane and dextran sodium sulfate. Cancer Sci 2003;94(11):965-73.
[49] Li Y, Liu J, Liu G, Pan Z, Zhang M, Ma Y, Wei Q, Xia H, Zhang RX, She J. Murine Appendectomy Model of Chronic Colitis Associated Colorectal Cancer by Precise Localization of Caecal Patch. J Vis Exp 2019(150).
[50] Kimura S, Yamakami-Kimura M, Obata Y, Hase K, Kitamura H, Ohno H, Iwanaga T. Visualization of the entire differentiation process of murine M cells: suppression of their maturation in cecal patches. Mucosal Immunol 2015;8(3):650-60.
[51] Cheung EC, Athineos D, Lee P, Ridgway RA, Lambie W, Nixon C, Strathdee D, Blyth K, Sansom OJ, Vousden KH. TIGAR is required for efficient intestinal regeneration and tumorigenesis. Dev Cell 2013;25(5):463-77.
[52] Caporaso JG, Lauber CL, Walters WA, Berg-Lyons D, Lozupone CA, Turnbaugh PJ, Fierer N, Knight R. Global patterns of 16S rRNA diversity at a depth of millions of sequences per sample. Proc Natl Acad Sci U S A 2011;108 Suppl 1(Suppl 1):4516-22.
[53] Callahan BJ, McMurdie PJ, Rosen MJ, Han AW, Johnson AJ, Holmes SP. DADA2: High-resolution sample inference from Illumina amplicon data. Nat Methods 2016;13(7):581-3.
[54] Quast C, Pruesse E, Yilmaz P, Gerken J, Schweer T, Yarza P, Peplies J, Glockner FO. The SILVA ribosomal RNA gene database project: improved data processing and web-based tools. Nucleic Acids Res 2013;41(Database issue):D590-6.
[55] McMurdie PJ, Holmes S. phyloseq: an R package for reproducible interactive analysis and graphics of microbiome census data. PLoS One 2013;8(4):e61217.
[56] Segata N, Izard J, Waldron L, Gevers D, Miropolsky L, Garrett WS, Huttenhower C. Metagenomic biomarker discovery and explanation. Genome Biol 2011;12(6):R60.
[57] Repass J, Maherali N, Owen K. Registered report: Fusobacterium nucleatum infection is prevalent in human colorectal carcinoma. Elife 2016;5.

[58] Iebba V, Santangelo F, Totino V, Nicoletti M, Gagliardi A, De Biase RV, Cucchiara S, Nencioni L, Conte MP, Schippa S. Higher prevalence and abundance of Bdellovibrio bacteriovorus in the human gut of healthy subjects. PLoS One 2013;8(4):e61608.
[59] https://www.bu.edu/researchsupport/compliance/animal-care/working-with-animals/research/sample-size-calculations-iacuc/.

Acknowledgements

We thank Nathalie Colnot, Raphaelle Liquard, Ian Morilla, Arielle Pierre, Olivier Thibaudeau and Laure Wingertsmann for their substantial contribution to this project. We are grateful to the INRAE MIGALE bioinformatics facility (MIGALE, INRAE, 2020. Migale bioinformatics Facility, doi: 10.15454/1.5572390655343293E12) for providing help and computing and storage resources.

Figures: titles and legends

Figure 1: Appendectomy increases tumorigenesis of CAC and reduces colitis severity.

(A) Experimental schema of the AOM/DSS protocol used to induce CAC in mice. At the end of the AOM/DSS protocol (12 weeks after surgery and AOM injection), the entire colon from each mouse was removed and open longitudinally. (B) Representative picture of an opened colon for each group (distal part of the colon on the right side). (C) Tumor quantification in the appendectomy (n=16) and control (n=10) groups (macroscopic examination). Colons were fixed and embedded in paraffin and prepared as "Swiss rolls". (D) Representative histological picture of a paraffin-embedded section stained with H&E reagent. (E) The number of tumors (microscopic examination) was counted in both groups. (F) Experimental schema of the DSS-only protocol. (G) Body weight evolution in the appendectomy (n=15) and control (n=15) groups during the DSS-only protocol (means). At the end of the DSS-only protocol, the entire colon was taken and stained with H&E reagent. Aperio ImageScope software was used to calculate the percentage of inflamed colonic epithelium surface within the entire colonic epithelium for each mouse. Comparison of the colon length (H) and of colitis extent (I) after the DSS-only protocol between the appendectomy and control groups. In all dot plots, the error bars represent the 25^{th}, 50^{th} (median) and 75^{th} interquartile ranges. Comparisons of 2 groups were performed using the Mann-Whitney test with 2-tailed p-value. A p-value <0.05 was considered statistically significant.

Figure 2: Relationship between the severity of DSS-induced colitis and the number of colonic tumors.

Four groups of mice were subjected to the AOM/DSS protocol without surgical intervention and treated with different DSS concentrations: 0.5% (n=9), 1.0% (n=10), 1.5% (n=10) and 2.0% (n=9). Mice were sacrificed 12 weeks after AOM injection. (A) Body weight evolution during

each DSS cycle in the 4 groups (means). (B) Macroscopic quantification of colonic tumors in each group. (C) Microscopic quantification of colonic tumors from H&E-stained slides. In all dot plots, the error bars represent the 25th, 50th (median) and 75th interquartile ranges. Comparisons of multiple groups were performed using the Kruskal-Wallis's test. A p-value <0.05 was considered statistically significant.

Figure 3: Transcriptome analysis of tumors, and assessment of tumor proliferation and fecal microbiota after appendectomy.

To perform a transcriptome analysis of CAC, 11 mice were subjected to the AOM/DSS protocol with appendectomy (n=6) or sham laparotomy (n=5). Colonic tumors from each mouse were pooled and mRNA expression was analyzed by microarray using GeneChip® MouseGene2.0ST (Affymetrix). Only transcripts with a p-value <0.05 and an expression threshold >1.5 were considered differentially expressed between appendectomized and control mice. (A) Vulcano plot used in the differential gene expression analysis. The colored dots (green and red) represent the genes differentially expressed based on a p-value <0.05 (False Discovery Rate=2%; represented by a black hashed horizontal line) and a 1.5-fold expression difference (represented by two black hashed vertical lines). (B) Representative immunohistochemistry with the anti-PCNA antibody (Sc-56, Biotechnology, 1/100 dilution) of colonic tumors from control and appendectomized mice treated with AOM/DSS. (C) Relative abondance of the 7 most represented bacterial phyla in fecal samples of mice that underwent appendectomy (n=5) or sham laparotomy (n=5). The V4 variable region of the 16S rRNA genes was amplified by PCR in each sample and sequenced. The taxonomy of each filtered sequence was assigned using the 16S rRNA database Silva 138.1. (D) Comparison of fecal microbiota alpha diversity assessed for richness (Chao1) and diversity (Shannon) between the appendectomy and control groups. Comparison of beta diversity according to the abundance

determined using (E) the Bray-Curtis or (F) the Jaccard index between both groups. (G) Cladogram generated by LEfSe (Linear discriminant analysis Effect Size) assessing differences in taxa of fecal microbiota between appendectomy and control. Regions in red indicate taxa that were enriched in the appendectomy group, white regions show no statistical differences and green regions would have referred to taxa enriched in the control group, but no significant differences found on this comparison. A p-value <0.05 was considered statistically significant.

Figure 4: *Fusobacterium nucleatum* intra-tumor infiltration is not influenced by appendectomy.

(A) Result of double PCR using Fusobacterium-specific primers in tumor DNA samples. M, DNA ladder; lanes 1-16, PCR products from tumor DNA samples; +, PCR product from Fusobacterium DNA; -, template without DNA. (B) Melting curves of q-PCR amplicons obtained using Fusobacterium-specific primers in tumor samples. Blue lines, amplicons from tumor DNA samples; green line, amplicon from Fusobacterium DNA; red line, template without DNA.

Figure 5: Appendectomy significantly alters intra-tumor T-cell immunity in mice.

Paraffin-embedded sections of the colon from each mouse taken at the AOM/DSS protocol endpoint in the appendectomy (n=16) and control (n=10) groups were stained with anti-CD3 or anti-CD8 antibodies. (A) Representative CD3+ cell immunostaining of colonic tumors after appendectomy or sham laparotomy (control). (B) Quantification of intra-tumor CD3+ T-cell density by an automated observer-independent process using Aperio ImageScope software in the appendectomy and control groups. (C) Representative CD8+ immunostaining of colonic tumors after appendectomy or sham laparotomy (control). (D) Quantification of intra-tumor CD8+ T-cell density in the appendectomy and control groups. All colonic tumors from

individual mice of the appendectomy (n=13) and control (n=12) groups subjected to the AOM/DSS protocol were resected and pooled. Intra-tumor CD3+ T-cells were isolated. Flow cytometry was performed to label CD3, CD4, CD8, CD62L, CD44 and PD1. Dot plots comparing intra-tumor cell labelling between the two groups in terms of (E) percentage of CD3+CD44^{high} cells among CD3+ cells, (F) CD62L^{low}/CD62L^{high} ratio among CD3+CD44^{high} cells, (G) percentage of PD1^{high} among CD3+ cells, (H) percentage of CD4+CD44^{high} cells among CD4+ cells, (I) CD62L^{low}/CD62L^{high} ratio among CD4+CD44^{high} cells, (J) percentage of PD1^{high} among CD4+ cells, (K) percentage of CD8+CD44^{high} cells among CD8+ cells, (L) CD62L^{low}/CD62L^{high} ratio among CD8+CD44^{high} cells, (M) percentage of PD1^{high} among CD8+ cells. (N) Scatter plot of CD3+ cells isolated from appendectomy and control mice stained for CD62L (x-axis) and for CD44 (y-axis). The red number represents the percentage of labeled cells. (O) T cells were isolated from pooled colonic tumors of individual mice subjected to the AOM/DSS protocol after appendectomy (n=13) and sham laparotomy (n=12). 100,000 cells per mouse were stimulated or not with a cocktail of PMA-ionomycin. The dot plot represents the production of TNF-alpha and IFN-gamma by stimulated T cells from the appendectomy and control groups measured by ELISA. In all dot plots, the error bars represent the 25th, 50th (median) and 75th interquartile ranges. Comparisons of 2 groups were performed using the Mann-Whitney test with 2-tailed p-value. A p-value <0.05 was considered statistically significant.

Figure 6: Effect of appendectomy on T-cell density after 3 DSS cycles (DSS-only protocol) and 1 week after surgery without DSS or AOM treatment (Surgery-only protocol).
Paraffin-embedded sections of the colon from each mouse after the DSS-only protocol in the appendectomy (n=15) and control (n=14 and not 15 due to a technical problem with one paraffin-embedded colon) groups were stained by immunohistochemistry (CD3 and CD8). (A)

Representative CD3+ cell staining of a colon after appendectomy or sham laparotomy (control). (B) Quantification of CD3+ T-cell density in the lamina propria in the appendectomy and control groups after the DSS-only protocol. (C) Representative CD8+ cell staining of a colon after appendectomy or sham laparotomy (control). (D) Quantification of CD8+ T-cell density in the lamina propria in the appendectomy and control groups after the DSS-only protocol. Paraffin-embedded sections of colons from mice sacrificed one week after surgery (appendectomy, n=7 or sham laparotomy, n=7) without AOM or DSS treatment (Surgery-only protocol) were stained by immunohistochemistry (CD3 and CD8). (E) Representative CD3+ cell staining of a colon after appendectomy or sham laparotomy (control). (F) Quantification of CD3+ T-cell density in the lamina propria in the appendectomy and control group after the Surgery-only protocol. (G) Representative CD8+ cell staining of a colon after appendectomy or sham laparotomy (control). (H) Quantification of CD8+ T-cell density in the lamina propria in the appendectomy and control groups after the Surgery-only protocol. (I) Picture of an isolated lymphoid follicle in the colon. (J) Number of isolated lymphoid follicles in the colon in the appendectomy and control groups after the Surgery-only protocol. In all dot plots, the error bars represent the 25th, 50th (median) and 75th interquartile ranges. Comparisons of 2 groups were performed using the Mann-Whitney test with 2-tailed p-value. A p-value <0.05 was considered statistically significant.

Figure 7: Blocking T-cell trafficking suppresses differences between appendectomized and no appendectomized mice.

(A-D) To block T-cell trafficking to the colon, an anti-integrin α4-β7 antibody was administered twice a week (125 μg/100 μL of InVivoMAb anti-mouse LPAM-1, BE0034, Bioxcell per injection) from the first day of the first DSS cycle to the end of the AOM/DSS protocol in mice that underwent appendectomy (n=9) or sham laparotomy (n=9). Intraperitoneal injections of

sterile PPB (100 µL) were performed following the same chronology in control group (n=8). At the AOM/DSS protocol endpoint, the colons were taken. Dot plots showing the comparisons between the appendectomy and sham groups in terms of (A) macroscopic number of tumors, (B) microscopic number of tumors, median intra-tumor CD3+ (C) and CD8+ (D) T-cell densities (immunohistochemistry). (E-H) To block T-cell trafficking to the colon, FTY720 (60 µg/100 µL per injection, SML0700, Sigma-Aldrich) was administered to 8 mice after appendectomy and to 9 mice after sham laparotomy following the AOM/DSS protocol and the frequency of injections was identical to that of the anti-integrin α4-β7 antibody. Intraperitoneal injections of sterile PPB (100 µL) were performed following the same chronology in control group (n=8). Dot plots showing the comparisons between the appendectomy and sham groups in terms of (E) macroscopic number of tumors, (F) microscopic number of tumors, median intra-tumor CD3+ (G) and CD8+ (H) T-cell densities (immunohistochemistry). In all dot plots, the error bars represent the 25^{th}, 50^{th} (median) and 75^{th} interquartile ranges. Comparisons of the three groups were performed using the Kruskal-Wallis test. Comparisons of 2 groups were performed using the Mann-Whitney test with 2-tailed p-value. A p-value <0.05 was considered statistically significant.

Figure 8: Appendicitis provides a partial protection against CAC and increases intra-tumor T-cell infiltration.

Neo-appendicitis was surgically induced in 10 mice without appendectomy and sham laparotomy was performed in 7 mice. These two surgical procedures were performed at Day 0 of the AOM/DSS protocol and mice were sacrificed 12 weeks later. The colons were taken for the following analyzes. Picture of the cecum (blue arrow) of a mice in the appendicitis group at the sacrifice (A). This picture highlights the presence of numerous peri-appendicular adhesions (red arrow) testifying to the local inflammation that occurs in this model of

appendicitis. (B) Tumor quantification in the appendicitis and control groups. (C) Number of tumors visible on the H&E-stained slides (microscopic examination). Paraffin-embedded sections from each mouse were stained by immunohistochemistry (CD3 and CD8). Intra-tumor CD3+ (D) and CD8+ (E) T-cell densities. To assess the impact of appendicitis on colitis, appendicitis induction (n=8) or sham laparotomy (n=7) was performed in mice subjected to the DSS-only protocol. (F) Body weight change during each DSS cycle of the DSS-only protocol in the appendicitis and control groups (means). At the end of the DSS-only protocol, mice were sacrificed and their colon was taken and paraffin-embedded sections were stained with H&E reagent. The percentage of inflamed colonic epithelium surface within the entire colonic epithelium was calculated for each mouse. (G) Comparison of colitis extent after the DSS-only protocol between the appendicitis and control groups. In all dot plots, the error bars represent the 25^{th}, 50^{th} (median) and 75^{th} interquartile ranges. Comparisons of 2 groups were performed using the Mann-Whitney test with 2-tailed p-value. A p-value <0.05 was considered statistically significant.

Figure 9: Injecting purified appendicular CD3+ or CD8+ T cells activated by appendicitis protects against CAC and increases intra-tumor T-cell infiltration.

One week after the surgical induction of neo-appendicitis in mice, inflamed appendices were resected, and appendicular cells were isolated. CD8+ cells, CD3+ cells, and CD45+ cells depleted in CD3+ cells were purified. $5x10^5$ living filtrated CD8+ T cells were injected into 8 mice (CD8+ T-cell injection group), $5x10^5$ living filtrated CD3+ T cells were injected into 8 mice (CD3+ T-cell injection group) and $5x10^5$ living filtrated CD45+ cells depleted in CD3+ T cells were injected into 8 mice (CD45+ CD3- cell injection group). All mice were subjected to the AOM/DSS protocol. (A) Macroscopic quantification of colonic tumors in each group. (B) Microscopic quantification of colonic tumors from H&E-stained slides. Paraffin-embedded

sections from each mouse were stained by immunohistochemistry (CD3 and CD8). Intra-tumor CD3+ (C) and CD8+ (D) T-cell densities quantified by an automated observer-independent process using Aperio ImageScope software. In all dot plots, the error bars represent the 25th, 50th (median) and 75th interquartile ranges. Comparisons of multiple groups were performed using the Kruskal-Wallis test and, only if the p-value was <0.05, multiple comparisons with post-hoc tests (Dunn's test) were performed. A p-value <0.05 was considered statistically significant.

Figure 10: Appendectomy significantly alters intra-tumor T-cell immunity in human CAC. Tumors from patients with ulcerative colitis who underwent surgical resection for CAC were analyzed. All paraffin blocks embedding the colorectal tumors were collected to perform immunohistochemistry (CD3 and CD8). Of the 24 tumors analyzed, 6 tumors were from patients with a history of appendectomy and 18 tumors were from patients without history of appendectomy (control group). (A) Representative expression of CD3 in human colonic tumors from patients who underwent or not (control) appendectomy. (B) Quantification of intra-tumor CD3+ T-cell density in the appendectomy and control human tumors. (C) Representative expression of CD8 in human colonic tumors from patients who underwent or not (control) appendectomy. (D) Quantification of intra-tumor CD8+ T-cell density in the appendectomy and control groups. In all dot plots, the error bars represent the 25th, 50th (median) and 75th interquartile ranges. Comparisons of 2 groups were performed using the Mann-Whitney test with 2-tailed p-value. A p-value <0.05 was considered statistically significant.

Table

Table 1. Characteristics of patients with ulcerative colitis who underwent surgical resection for colitis-associated cancer.

	History of appendectomy	No history of appendectomy	p-value
Population	n= 5	n= 16	
Gender (female *vs.* male)	0 (0)[1]/5 (100)	8 (50)/8 (50)	0.111
Age (years)	38 (28-64)[2]	49 (39-55)	0.603
Primary biliary cholangitis	0 (0)	4 (25)	0.532
Medical treatment for colitis in the 6 months before surgery	3 (60)	9 (56)	1.000
Colorectal cancer	n=6	n=18	
Location: right or transverse colon *versus* left colon/rectum,	3 (50)-2 (33)-1 (17)-0 (0)	7 (39)-1 (6)-6 (33)-4 (22)	0.197
T-stage[3]			0.539
-*In situ*	1 (17)	1 (6)	
-*1*	1 (17)	3 (16)	
-*2*	0 (0)	2 (11)	
-*3*	2 (33)	10 (56)	
-*4*	2 (33)	2 (11)	
N-stage: 0 / 1 or 2	4 (67)/2 (33)	14 (78)/4 (22)	0.618
M-stage: 0 / 1	6 (100)/0 (0)	18 (100)/0 (0)	1.000

[1]number of patients (percent); [2]median (interquartile range); [3]according to the 8th TNM classification

Figure 1

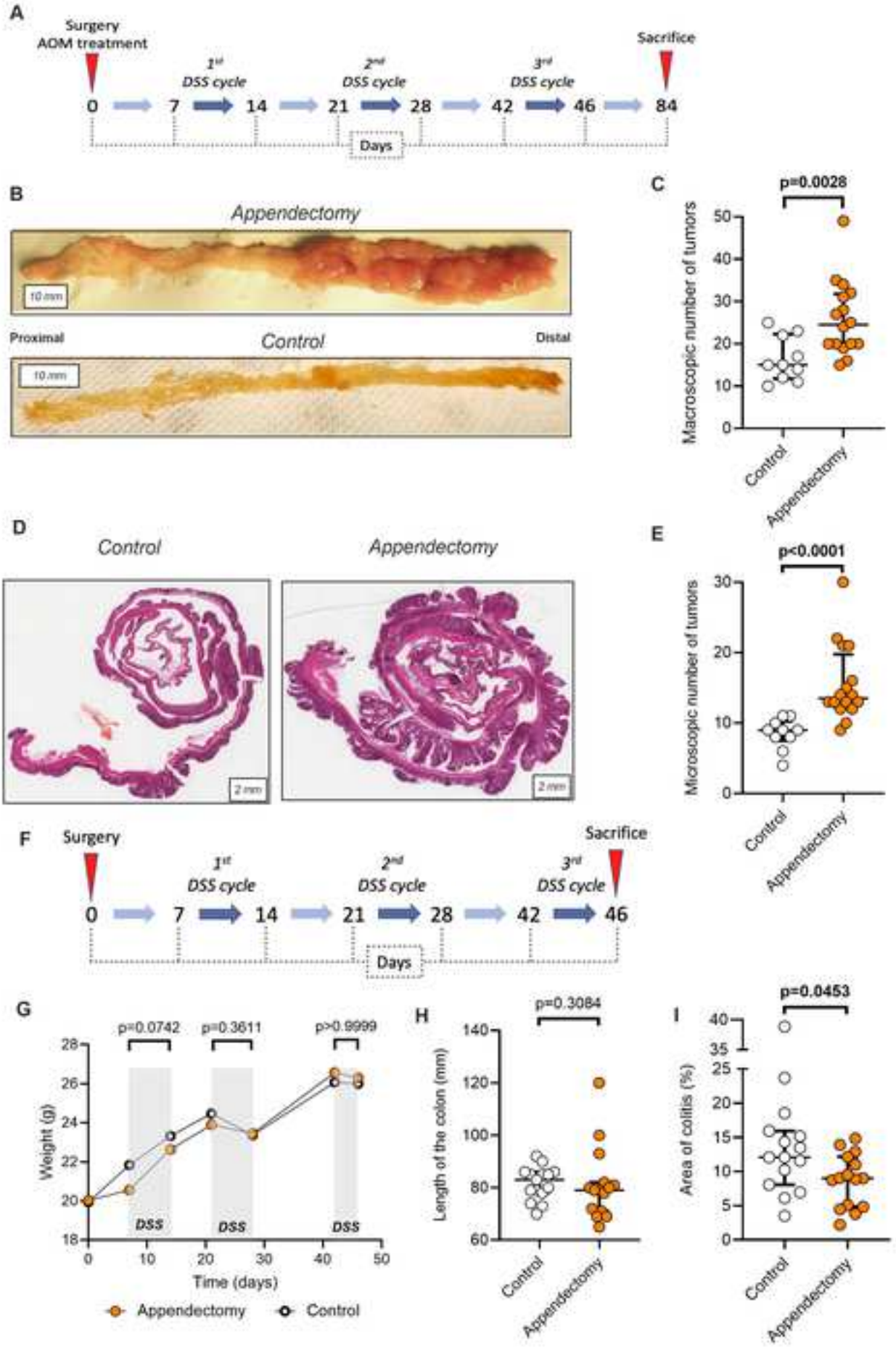

Figure 2

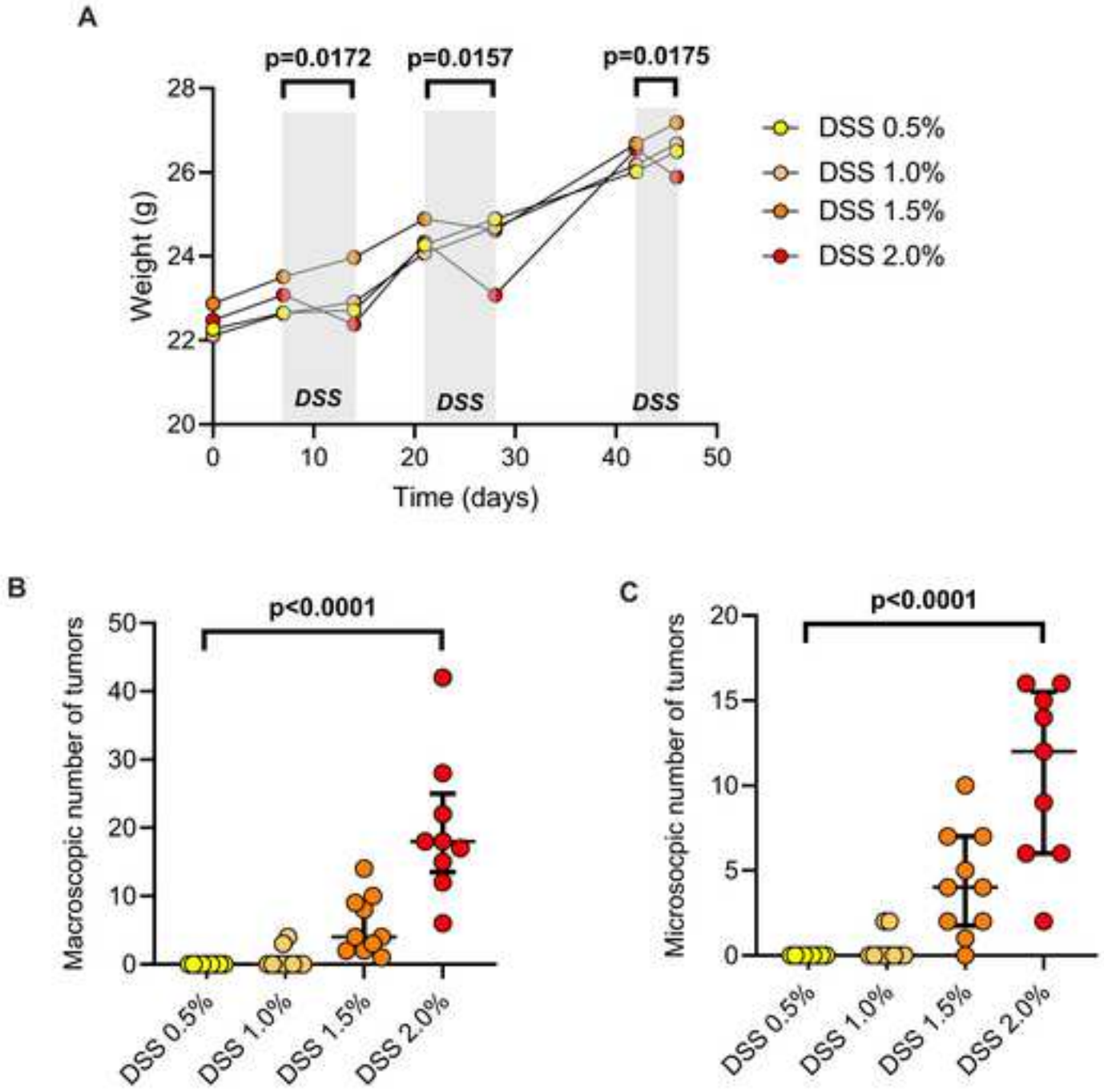

Figure 3

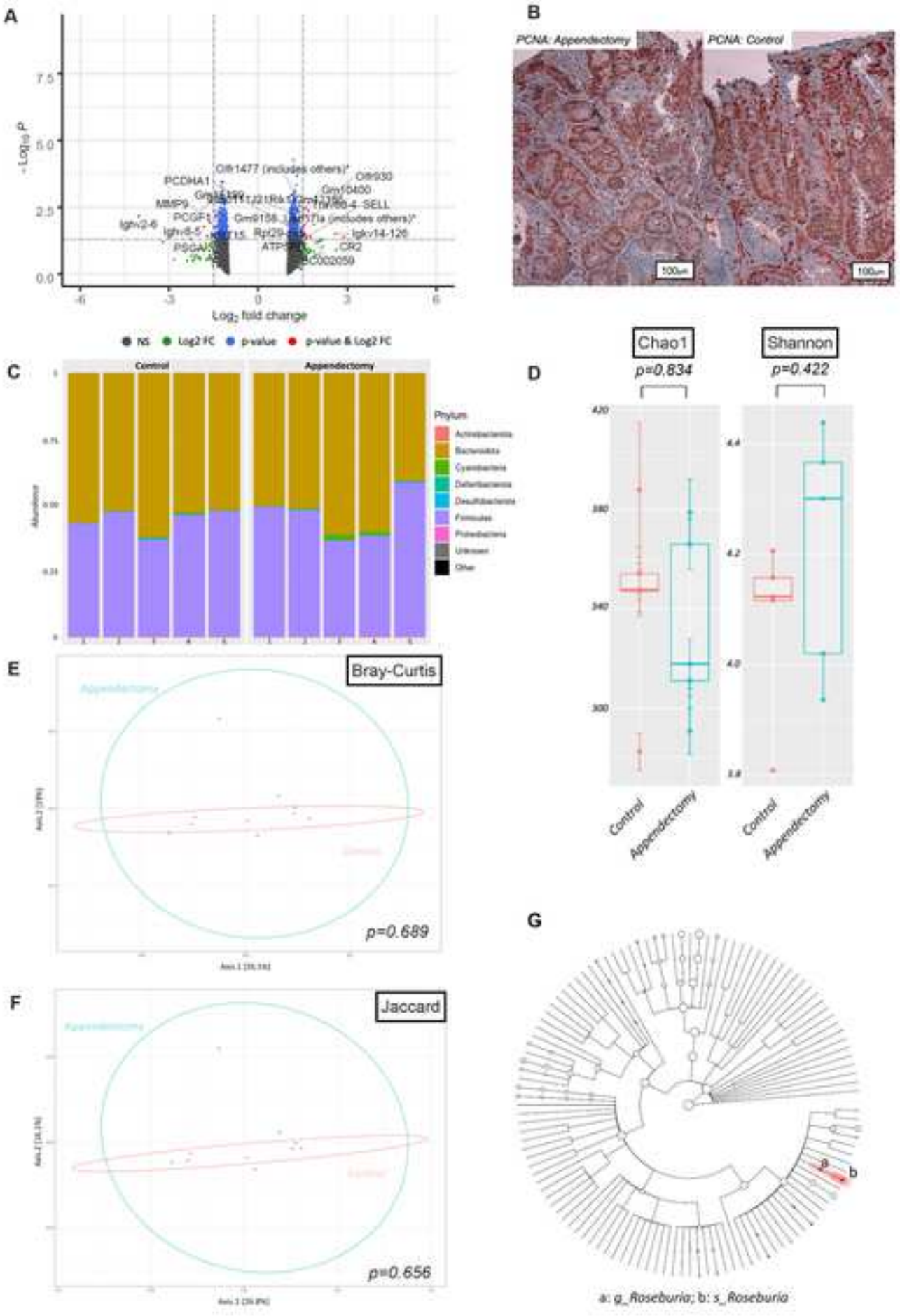

Figure 4

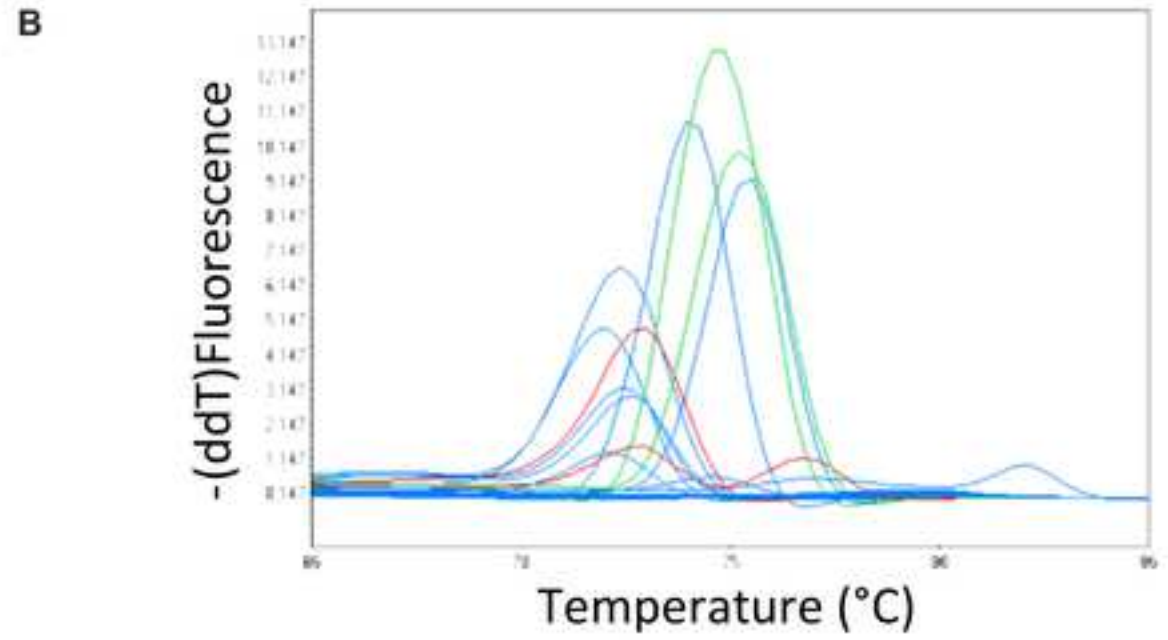

Figure 5

Click here to access/download;Figure;Figure 5.tif

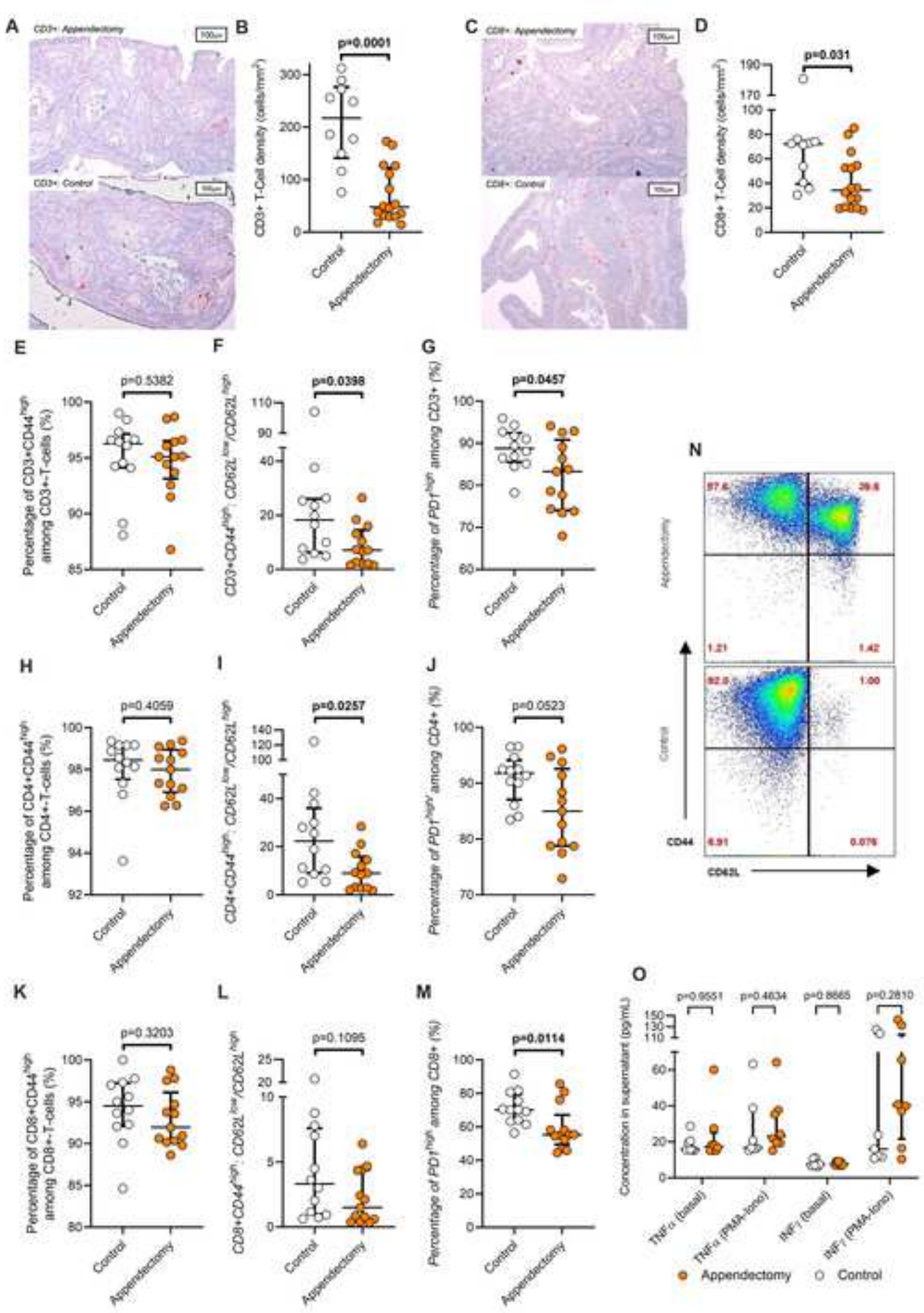

Figure 6

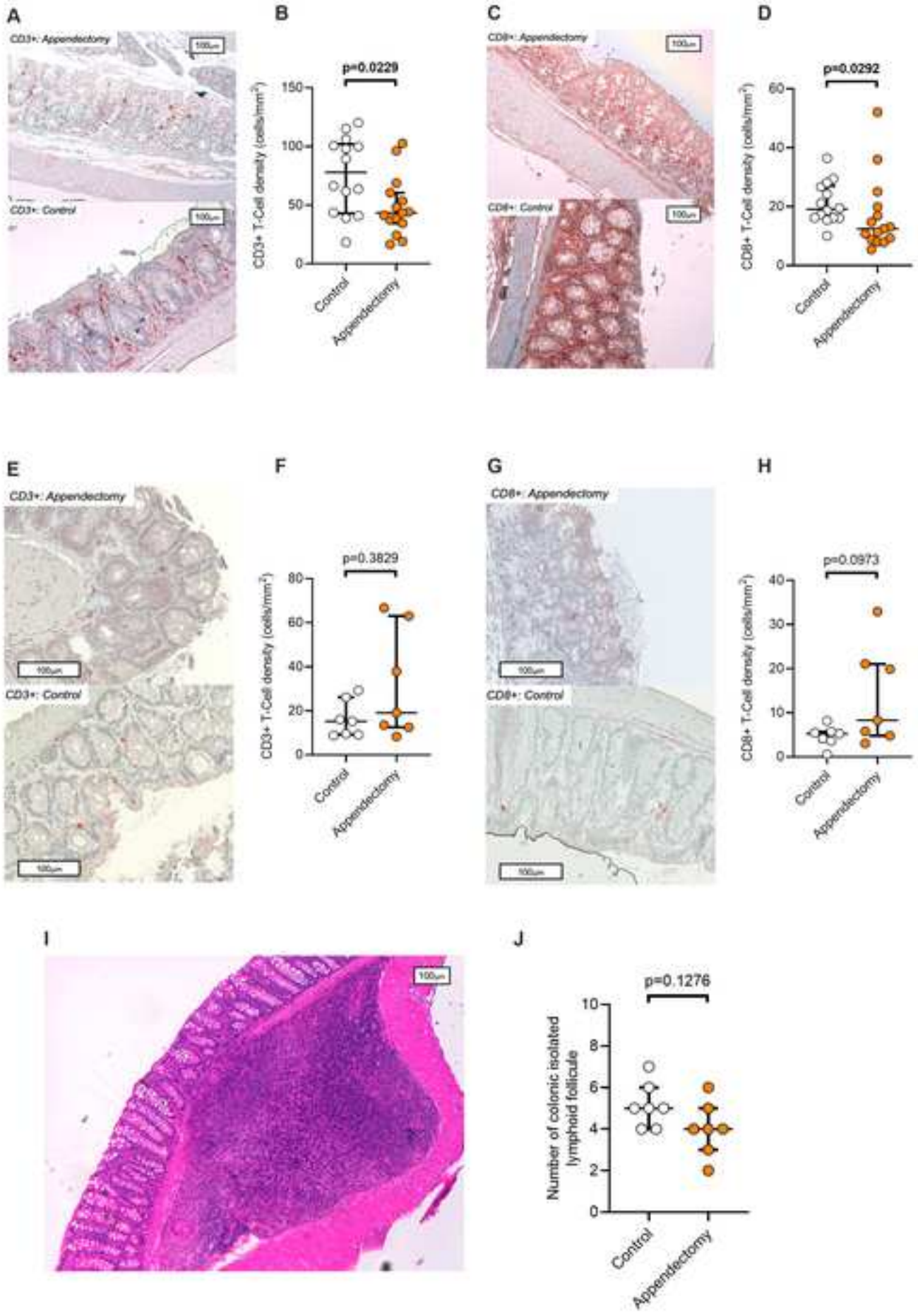

Figure 7

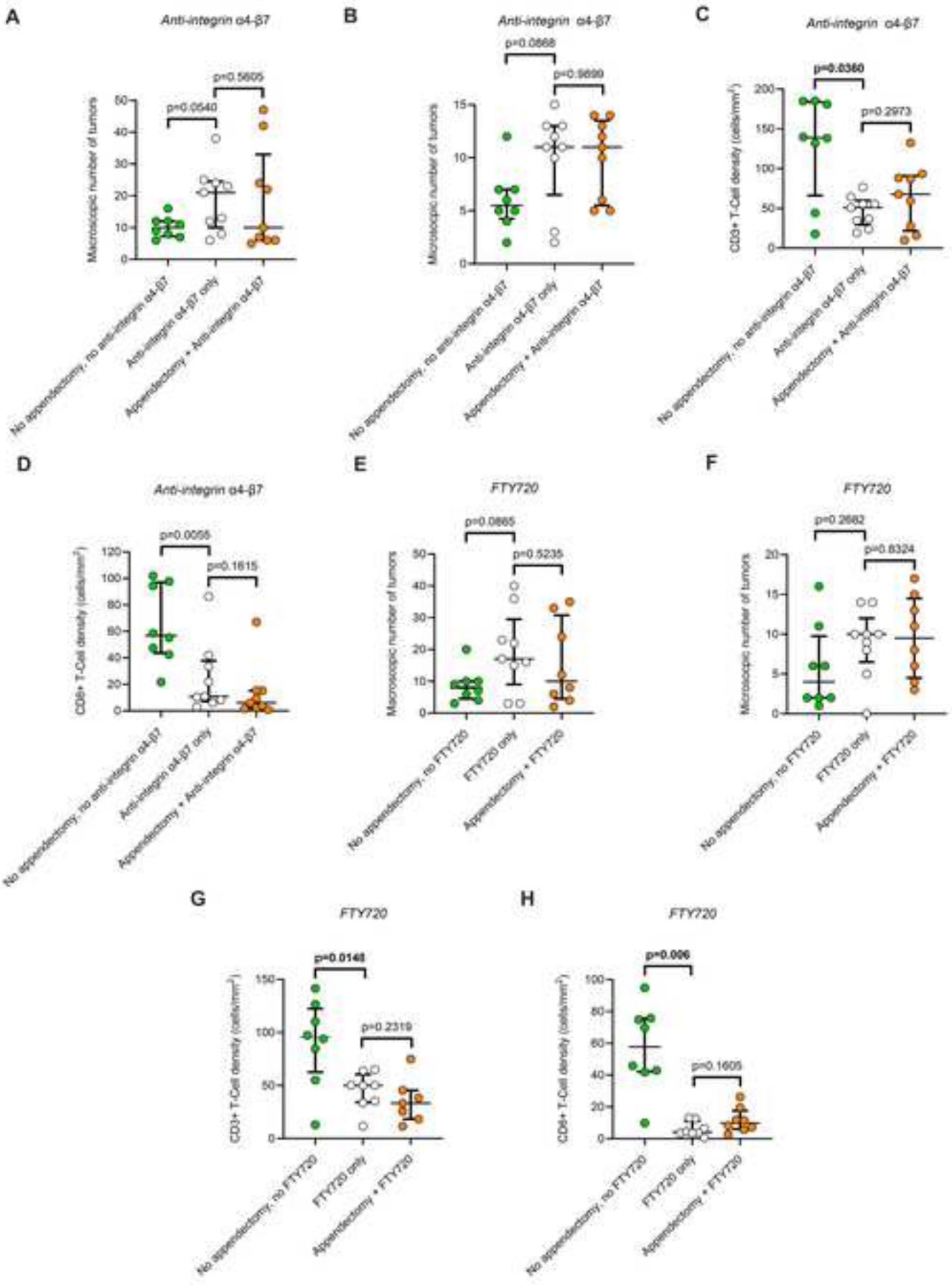

Figure 8

Click here to access/download;Figure;Figure 8.tif

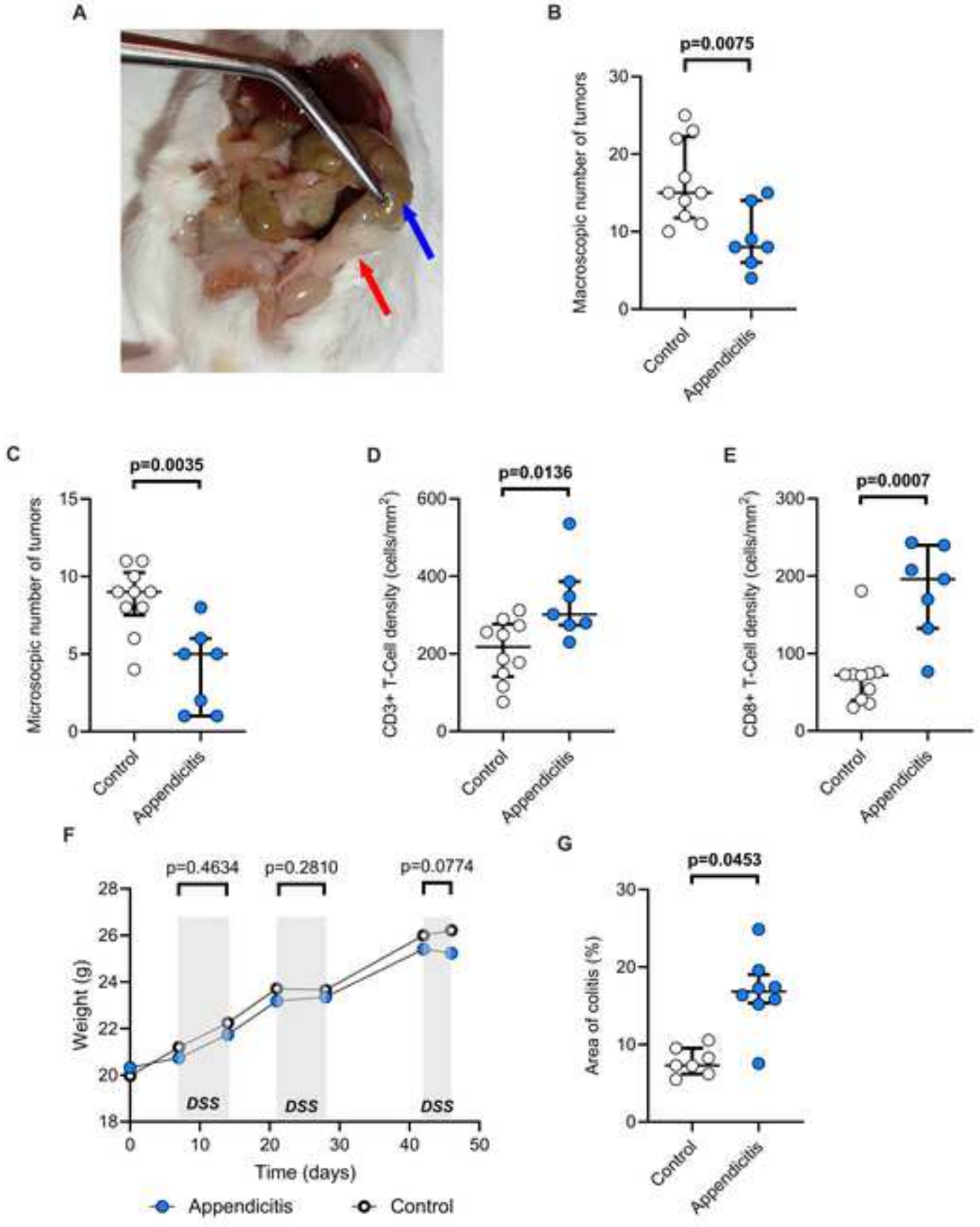

Figure 9

Click here to access/download;Figure;Figure 9.tif

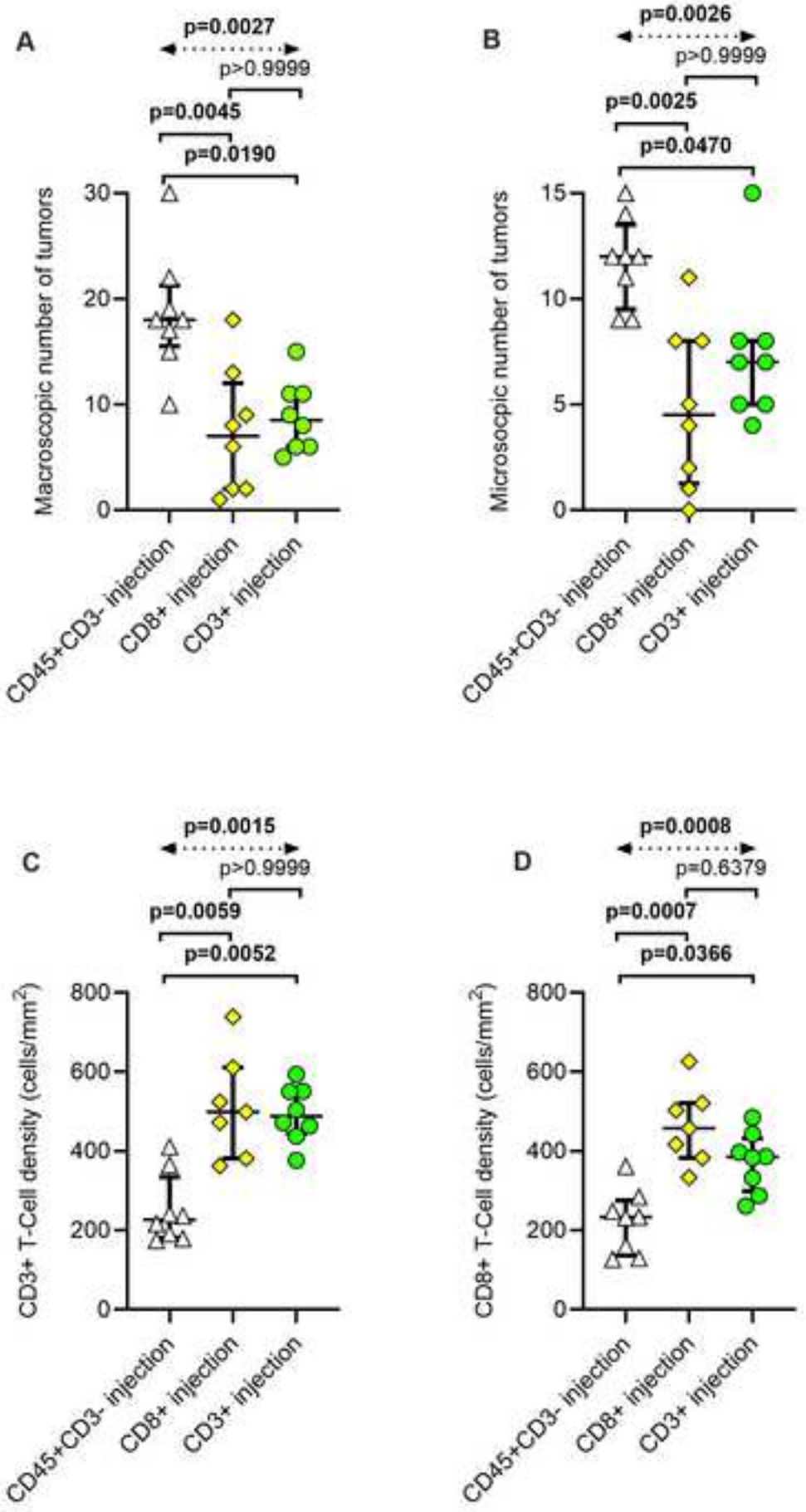

Figure 10

Click here to access/download;Figure;Figure 10.tif